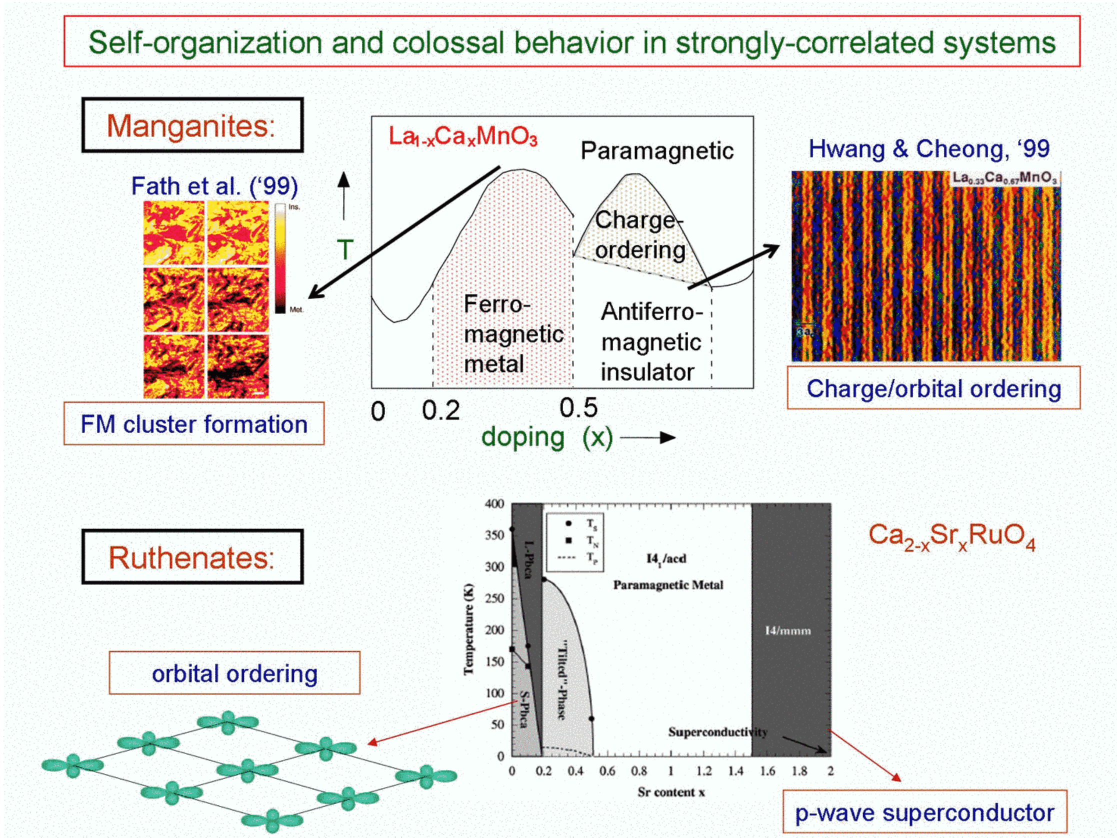
Self-organization and colossal behavior in strongly-correlated systems
Manganites:
Fath et al. ('99)
FM cluster formation
La1-xCaxMnO3
Paramagnetic
Charge-ordering
Ferro-magnetic metal
Antiferro-magnetic insulator
T
0 0.2 0.5
doping (x)
Hwang & Cheong, '99
Charge/orbital ordering
Ruthenates:
orbital ordering
Ca2-xSrxRuO4
I41/acd
Paramagnetic Metal
I4/mmm
L-Pbca
S-Pbca
"Tilted"-Phase
Superconductivity
Temperature (K)
Sr content x
p-wave superconductor

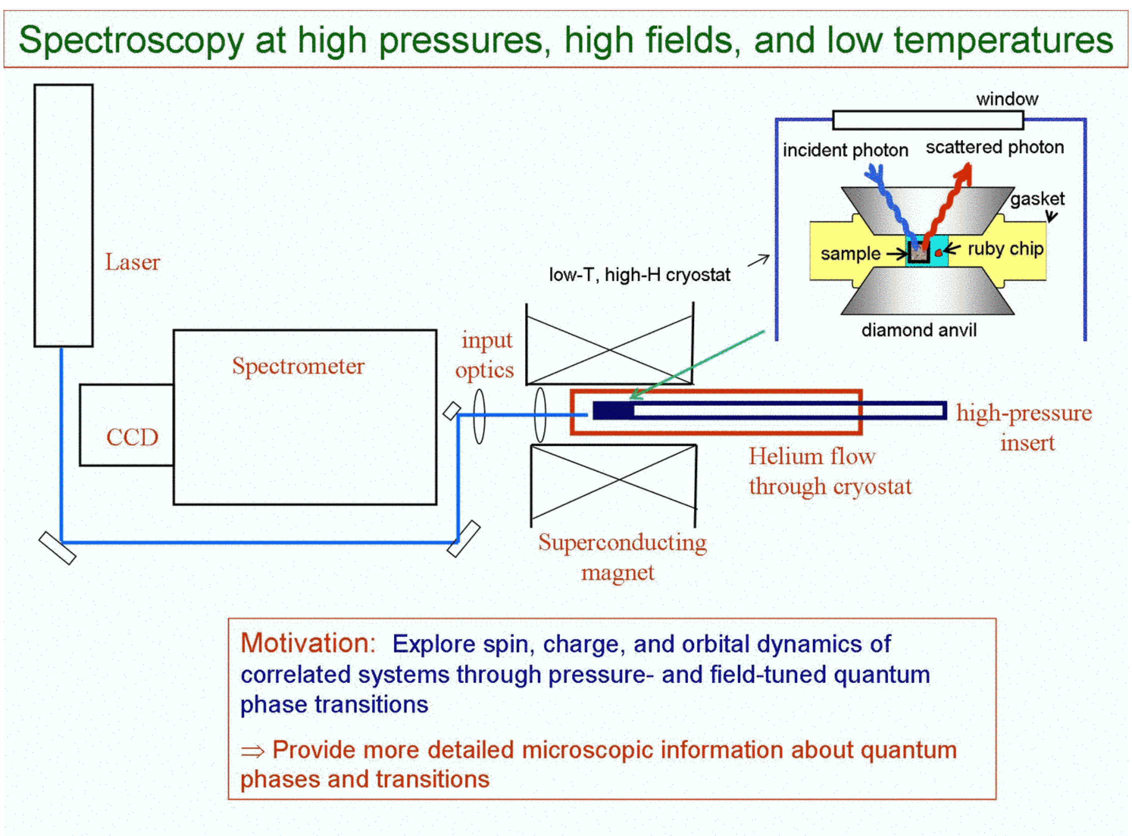
Spectroscopy at high pressures, high fields, and low temperatures
Laser
Spectrometer
CCD
input optics
low-T, high-H cryostat
window
incident photon
scattered photon
gasket
sample
ruby chip
diamond anvil
high-pressure insert
Helium flow through cryostat
Superconducting magnet
Motivation: Explore spin, charge, and orbital dynamics of correlated systems through pressure- and field-tuned quantum phase transitions
⇒ Provide more detailed microscopic information about quantum phases and transitions

Lessons from pressure- and field-induced spectroscopic studies of correlated materials: OUTLINE

(1). Cluster Formation and CMR in Eu-based compounds:

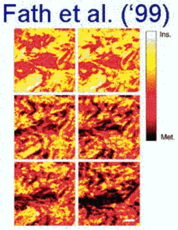

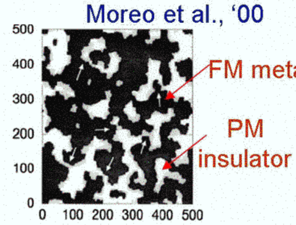

(2). Tuning the orbital states in layered ruthenates:

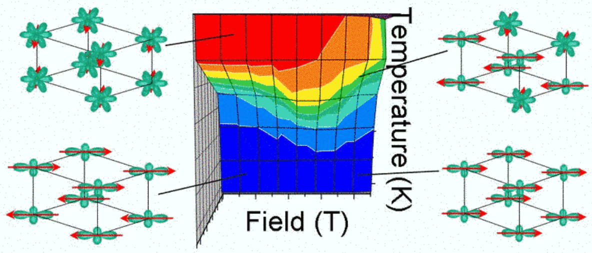

(3). Field- and pressure-induced melting of self-organized states in complex materials:

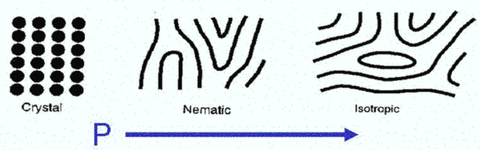

People who did the work:

Pressure-tuned Raman studies of ruthenates and CDW systems

Clark Snow (UIUC)

John Karpus (UIUC)

Pressure- and field-tuned Raman studies of ruthenates

Field- and pressure - tuned Raman studies of spin-lattice coupling in ruthenates, geometrically-frustrated systems

Dr. Rajeev Gupta (UIUC)

Field- and pressure-tuned Raman studies of manganites:

Minjung Kim (UIUC)

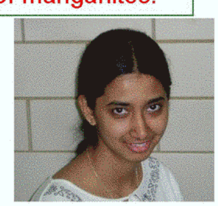

Harini Barath (UIUC)

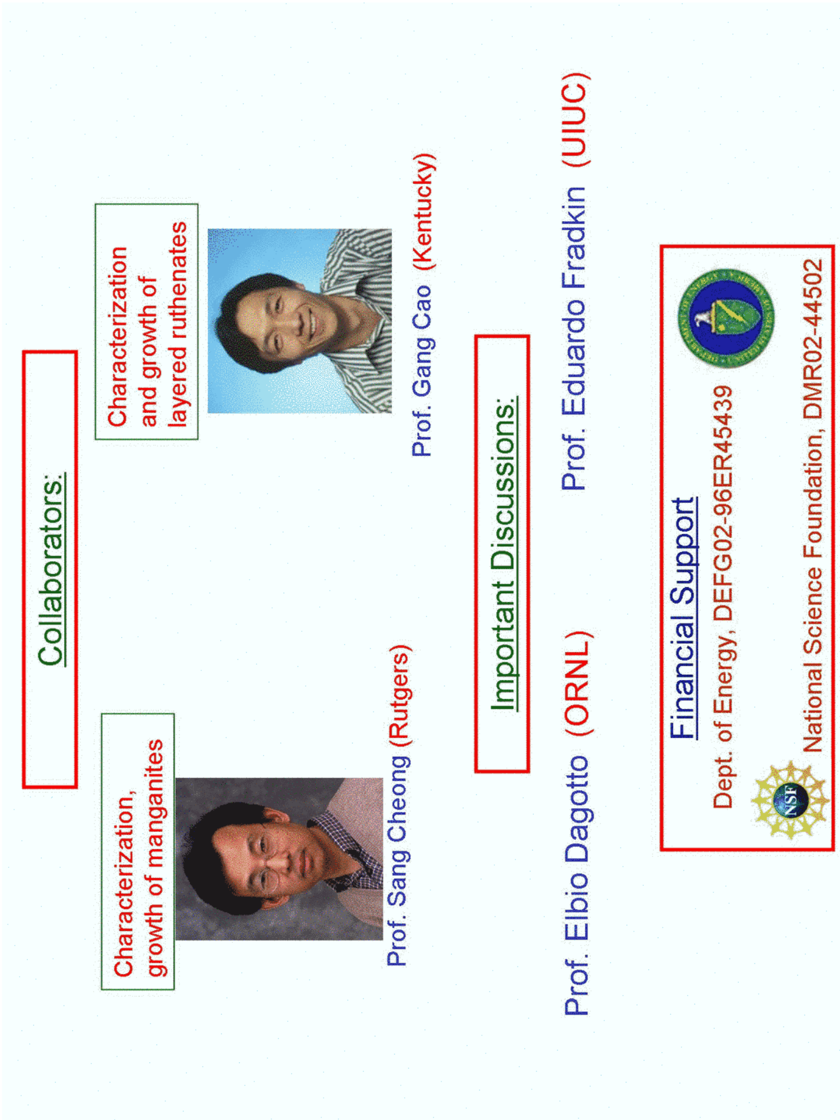

Collaborators:
Characterization, growth of manganites
Prof. Sang Cheong (Rutgers)
Characterization and growth of layered ruthenates
Prof. Gang Cao (Kentucky)
Important Discussions:
Prof. Elbio Dagotto (ORNL)
Prof. Eduardo Fradkin (UIUC)
Financial Support
Dept. of Energy, DEFG02-96ER45439
National Science Foundation, DMR02-44502

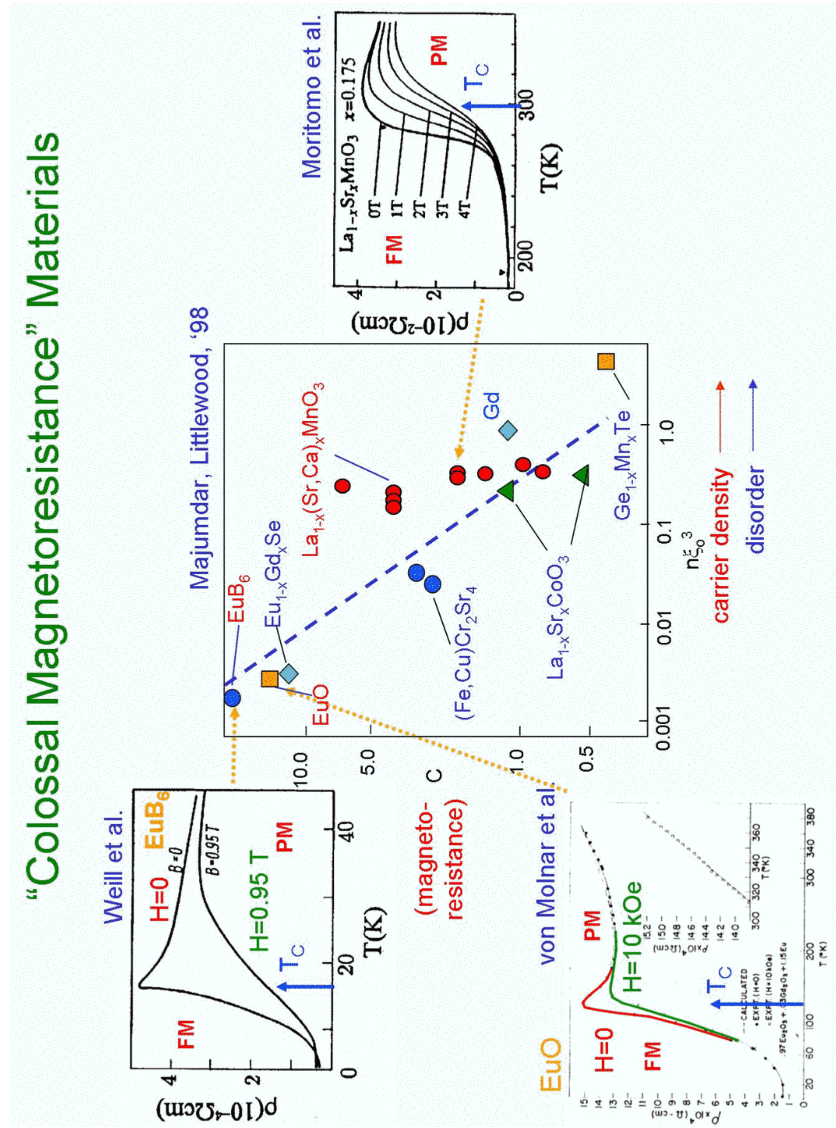

"Colossal Magnetoresistance" Materials
Majumdar, Littlewood, '98
Moritomo et al.
Weill et al.
von Molnar et al.
EuB6
EuO
Eu1-xGdxSe
La1-x(Sr,Ca)xMnO3
Gd
Ge1-xMnxTe
La1-xSrxCoO3
(Fe,Cu)Cr2Sr4
C (magneto-resistance)
carrier density
disorder
H=0
H=0.95 T
H=10 kOe
FM
PM
TC
T(K)
ρ(10-4Ωcm)
ρ(10-2Ωcm)

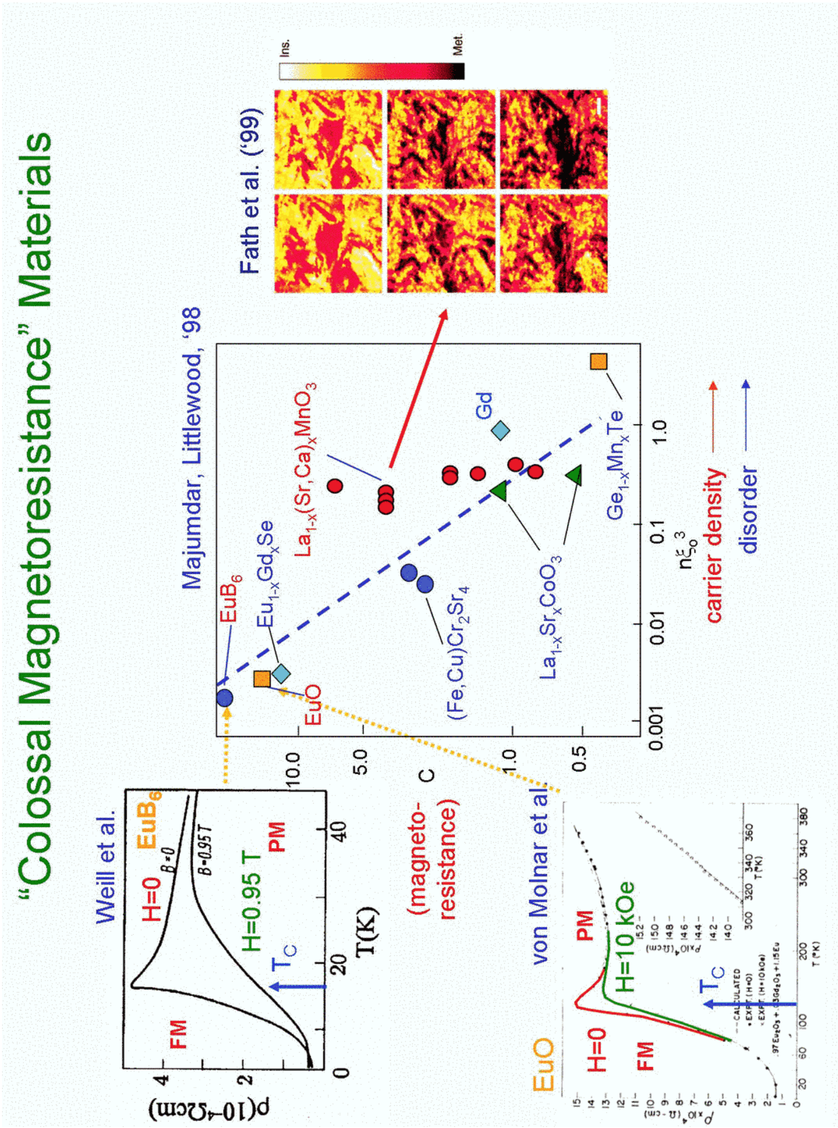
"Colossal Magnetoresistance" Materials
Majumdar, Littlewood, '98
Fath et al. ('99)
Ins.
Met.
Weill et al.
EuB$_6$
H=0
H=0.95 T
FM
PM
T$_C$
T(K)
ρ(10^{-4}Ωcm)
C
(magneto-resistance)
EuB$_6$
Eu$_{1-x}$Gd$_x$Se
EuO
La$_{1-x}$(Sr,Ca)$_x$MnO$_3$
Gd
(Fe,Cu)Cr$_2$Sr$_4$
La$_{1-x}$Sr$_x$CoO$_3$
Ge$_{1-x}$Mn$_x$Te
$n\xi_o^3$
carrier density
disorder
von Molnar et al.
EuO
H=0
H=10 kOe
FM
PM
T$_C$

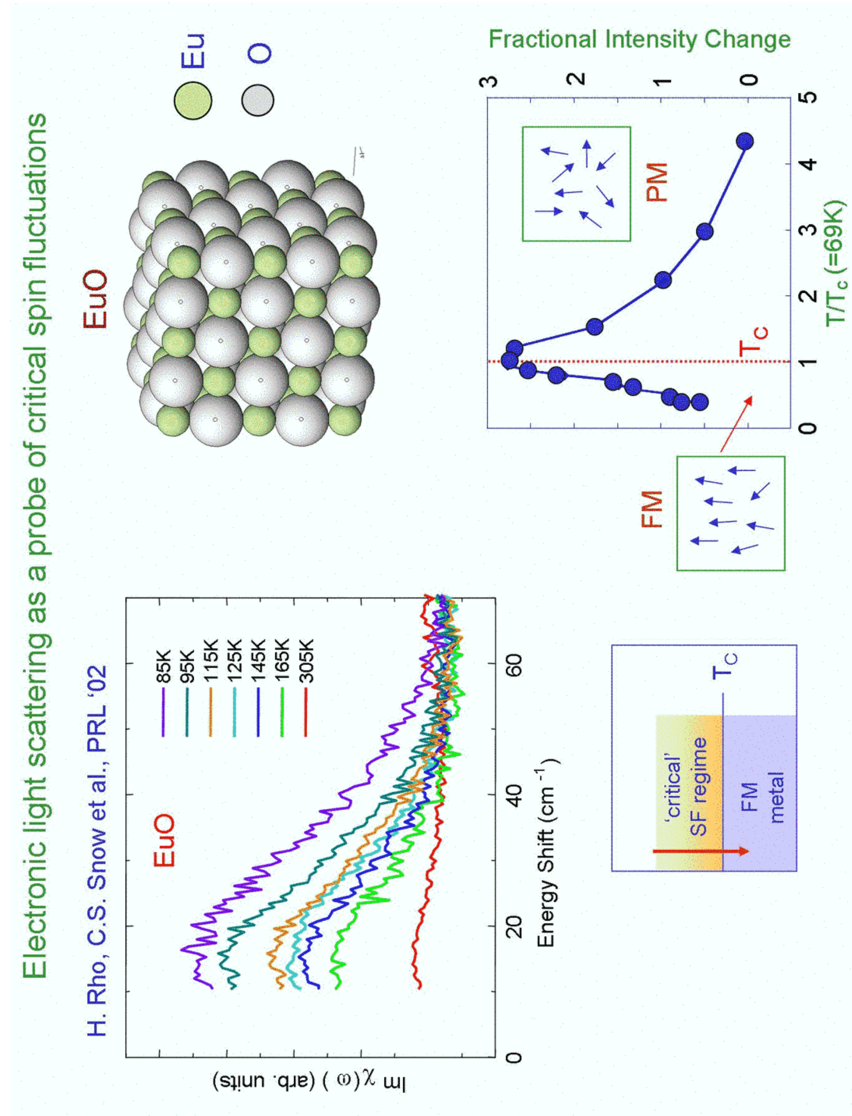
Electronic light scattering as a probe of critical spin fluctuations
H. Rho, C.S. Snow et al., PRL '02
EuO
Eu
O
85K
95K
115K
125K
145K
165K
305K
Im χ(ω) (arb. units)
Energy Shift (cm^{-1})
Fractional Intensity Change
T/T$_c$ (=69K)
T$_c$
FM
PM
'critical' SF regime
FM metal

Spin Cluster Formation in EuO

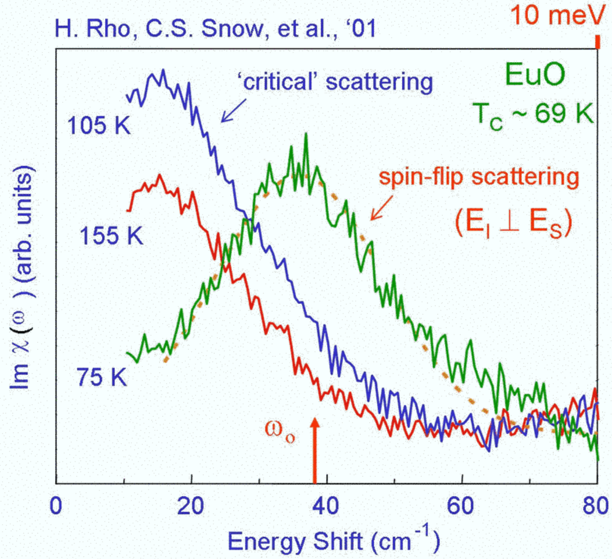

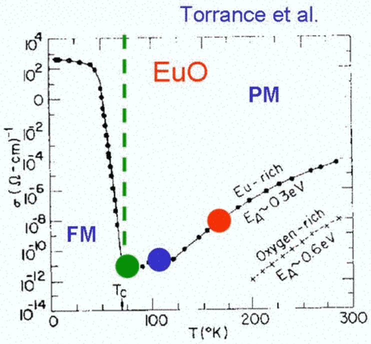

Spin Cluster Formation in EuO

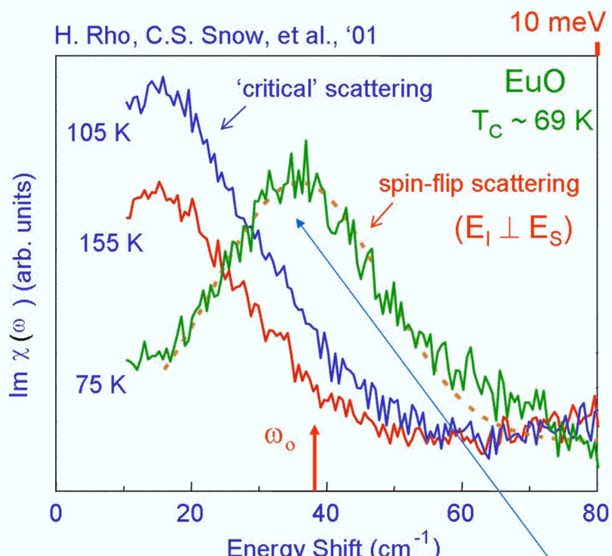

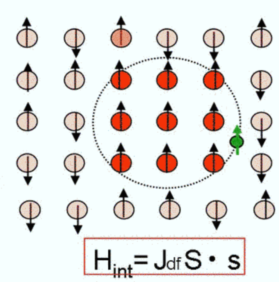

- "H=0 Zeeman splitting"

  $H_{eff} = \hbar\omega_o/g\mu_B$ ~ 50 - 100 T!

- energy reflects size of spin clusters

  J_{df} ~ 0.1 eV ⇒ ~ 20 - 40 spins (EuO)
  ~ 30 - 60 spins (EuB_6)

- gaussian profile reflects distribution of cluster sizes

$$\mathrm{Im}\,\chi \propto \frac{1}{w\sqrt{\frac{\pi}{2}}} Exp\left[-2\left(\frac{\omega-\omega_o}{w}\right)^2\right]$$

Why do they form? Energetically favorable to localize (and lose confinement energy ~ $\hbar^2/mr_o^2$) to gain exchange energy ~ $J_{df}\langle S\rangle$

Evolution of spin clusters into FM phase:

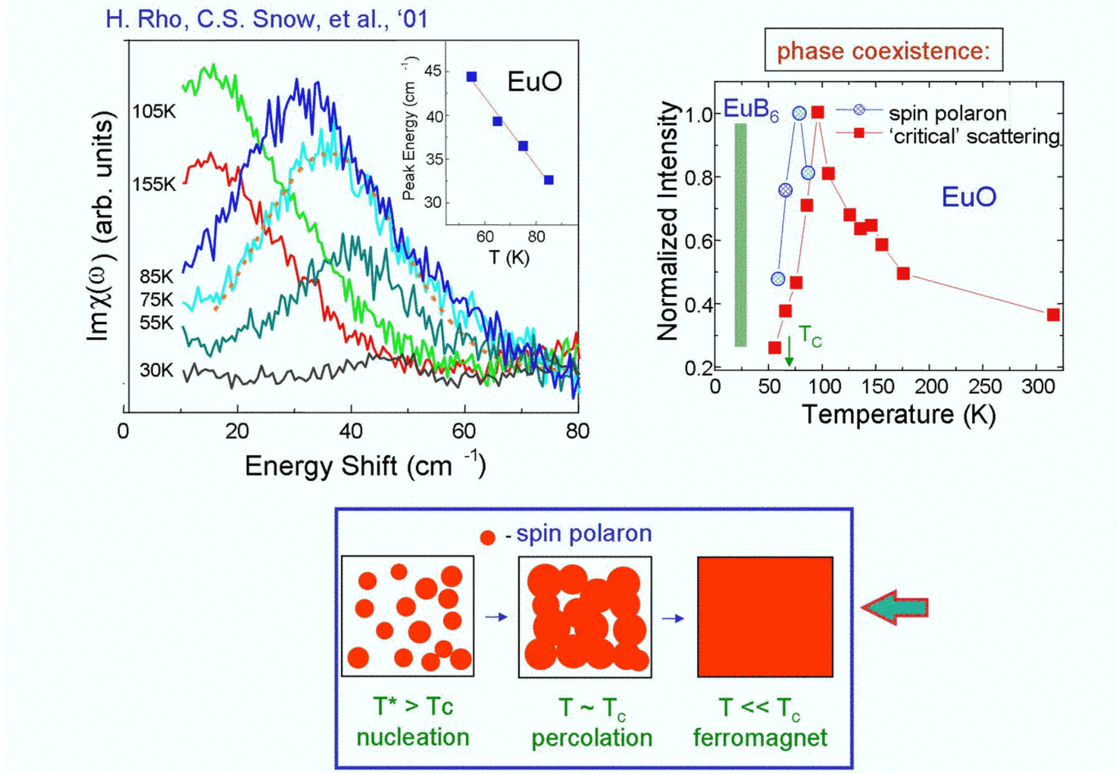

Field-induced nucleation of spin clusters

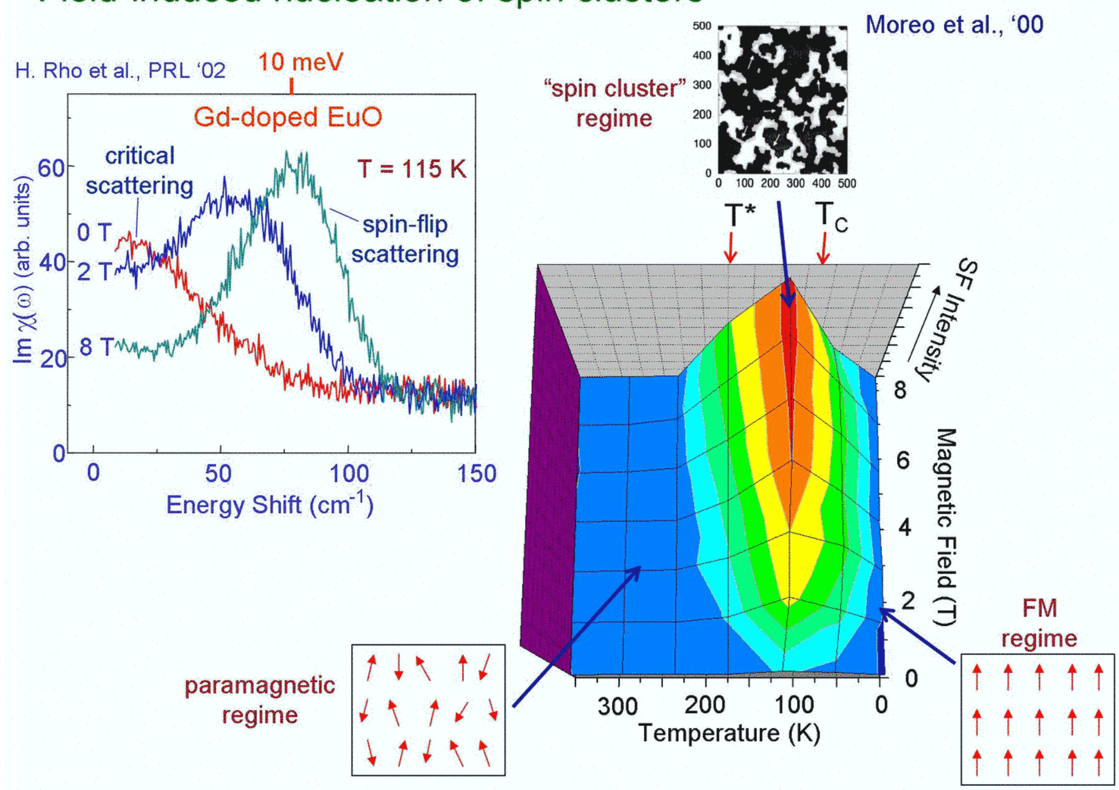

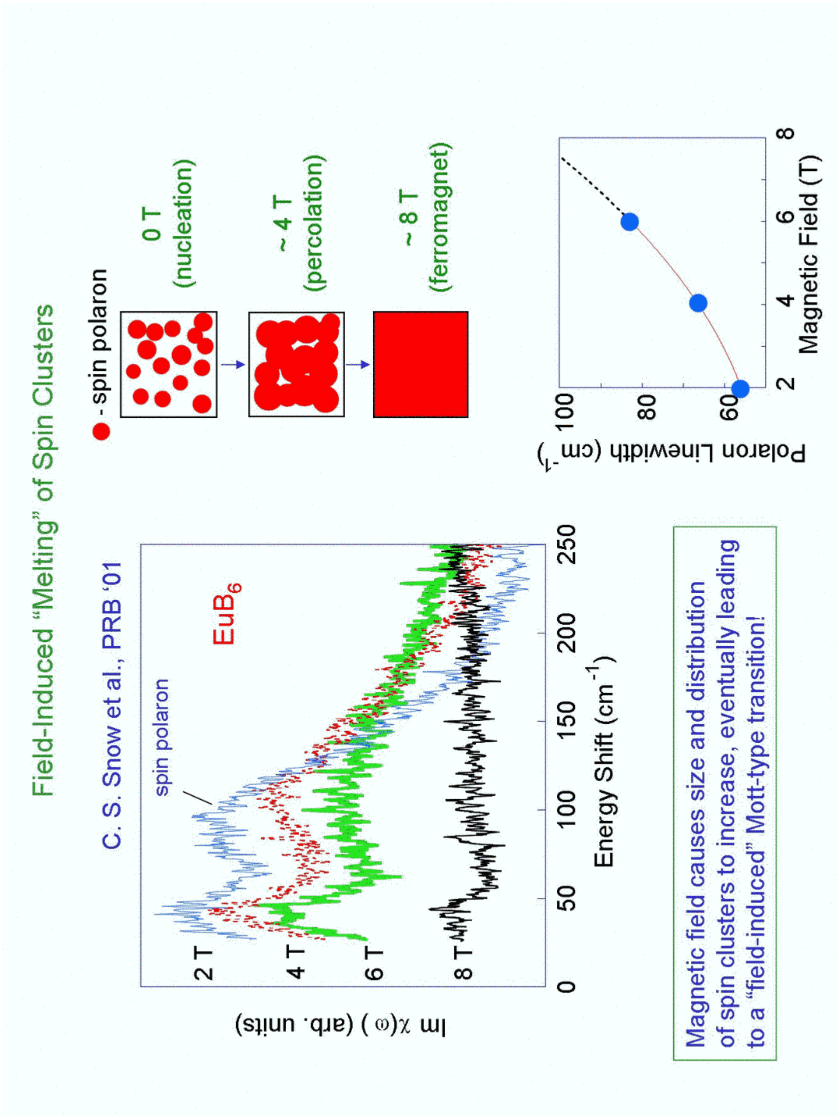

Field-Induced "Melting" of Spin Clusters
C. S. Snow et al., PRB '01
EuB$_6$
spin polaron
2 T
4 T
6 T
8 T
Im χ(ω) (arb. units)
Energy Shift (cm^{-1})
0
50
100
150
200
250
- spin polaron
0 T (nucleation)
~ 4 T (percolation)
~ 8 T (ferromagnet)
Polaron Linewidth (cm^{-1})
Magnetic Field (T)
Magnetic field causes size and distribution of spin clusters to increase, eventually leading to a "field-induced" Mott-type transition!

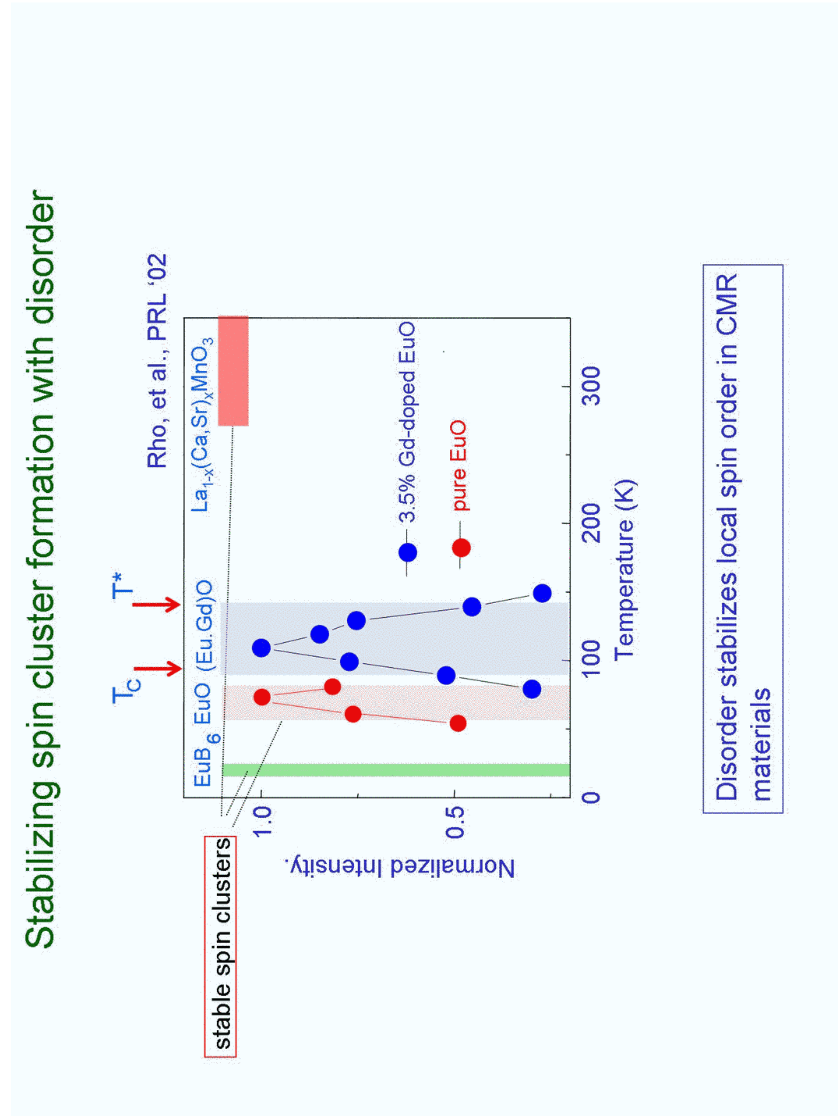

Stabilizing spin cluster formation with disorder
Rho, et al., PRL '02
T_C
T*
EuB$_6$
EuO
(Eu,Gd)O
La$_{1-x}$(Ca,Sr)$_x$MnO$_3$
3.5% Gd-doped EuO
pure EuO
Normalized Intensity
Temperature (K)
stable spin clusters
Disorder stabilizes local spin order in CMR materials

Colossal Field Effects: Disorder and the amplification of applied fields by spin clusters

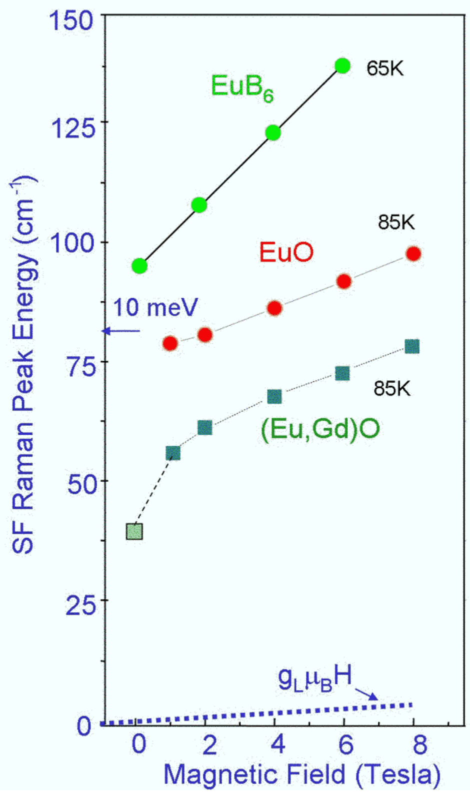

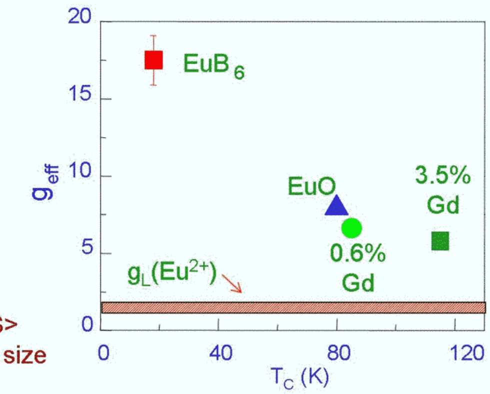

"Colossal Effects" induced by spin clusters:

- "amplification" of g-factor: ~ $E_{split}/\mu_B H$ (effects reduced by disorder)
- Abrupt field-induced percolation of clusters: "Field-induced" Mott Transition
- "Spin valve" effect? - cooperative effects induced by aligning clusters in small fields

Key results:

- Mesoscale cluster formation is ubiquitous in complex materials
- Disorder stabilizes local order
- Local order is key in generating "colossal" behavior

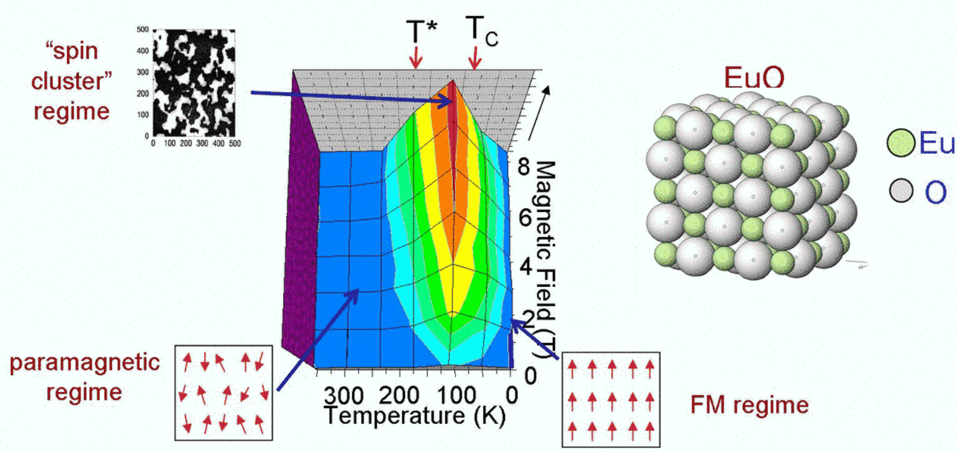

Topic 2: Pressure and field tunability of layered ruthenates

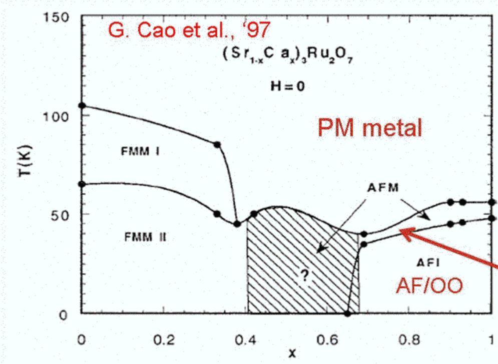

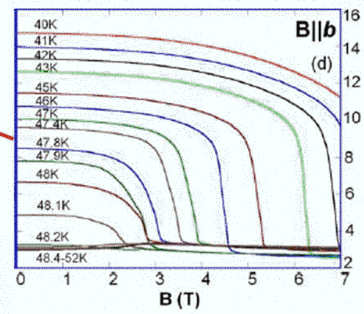

Cao et al., unpublished

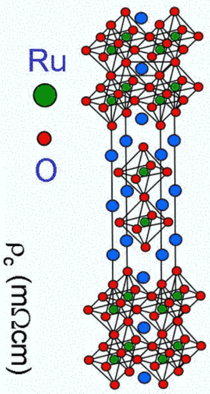

Key issues:

- Key role of orbital degree of freedom in complex materials
- Highly tunable behavior in complex materials
- Alternative routes for "colossal" behavior

Perovskite-related oxides with t_{2g}-orbital degeneracy

Ru^{4+}: t_{2g}^4

Key Features: Weak Hund's Coupling, $J_H < \Delta_{CF}$
⇒ effect of extended 4d orbitals in Ru
Spin-orbit coupling is important!

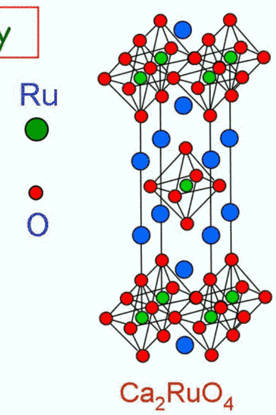

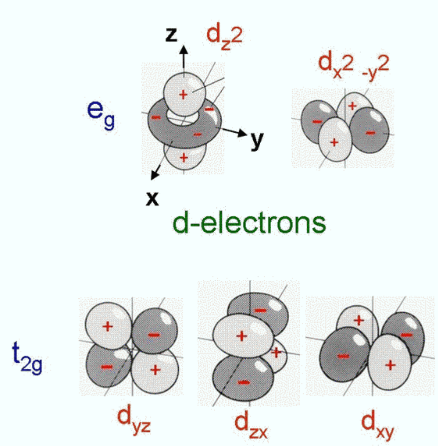

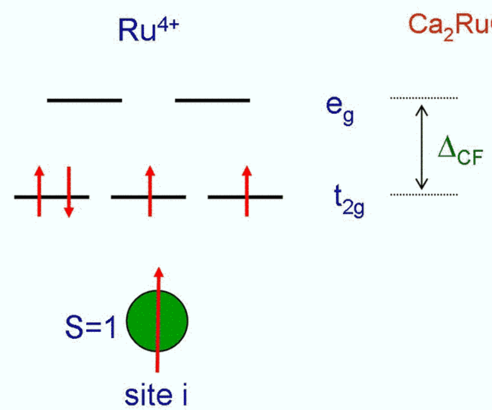

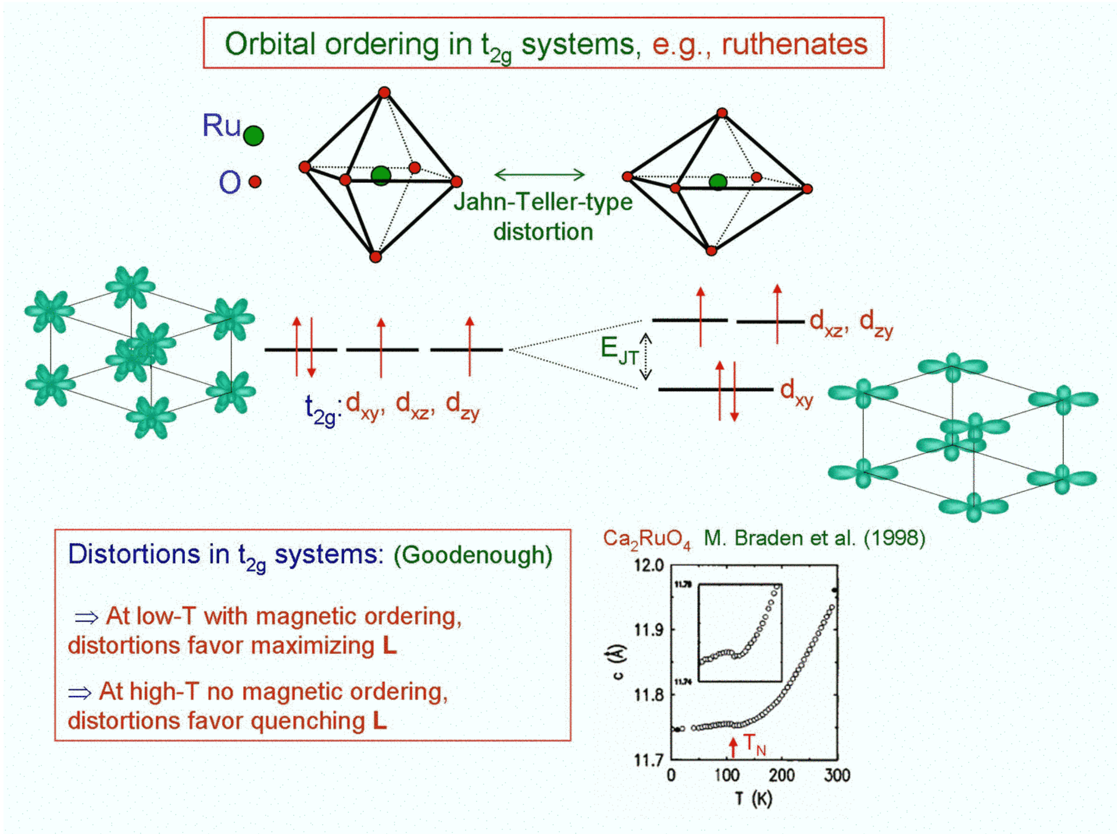
Orbital ordering in t_{2g} systems, e.g., ruthenates
Ru
O
Jahn-Teller-type distortion
t_{2g}: d_{xy}, d_{xz}, d_{zy}
E_{JT}
d_{xz}, d_{zy}
d_{xy}
Distortions in t_{2g} systems: (Goodenough)
⇒ At low-T with magnetic ordering, distortions favor maximizing **L**
⇒ At high-T no magnetic ordering, distortions favor quenching **L**
Ca_2RuO_4 M. Braden et al. (1998)
c (Å)
T_N
T (K)

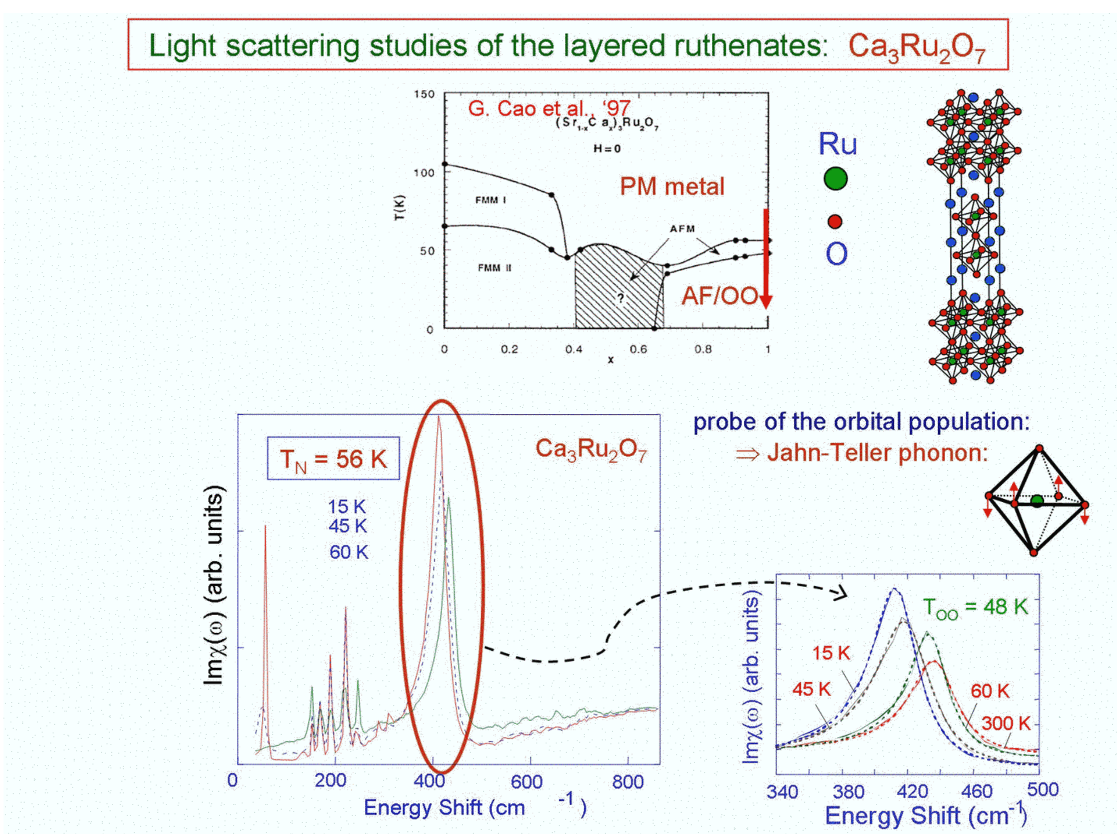
Light scattering studies of the layered ruthenates: $Ca_3Ru_2O_7$
G. Cao et al. '97
H = 0
PM metal
FMM I
FMM II
AFM
AF/OO
T(K)
x
Ru
O
T_N = 56 K
$Ca_3Ru_2O_7$
15 K
45 K
60 K
Imχ(ω) (arb. units)
Energy Shift (cm^{-1})
probe of the orbital population:
⇒ Jahn-Teller phonon:
T_{OO} = 48 K
15 K
45 K
60 K
300 K
Imχ(ω) (arb. units)
Energy Shift (cm^{-1})

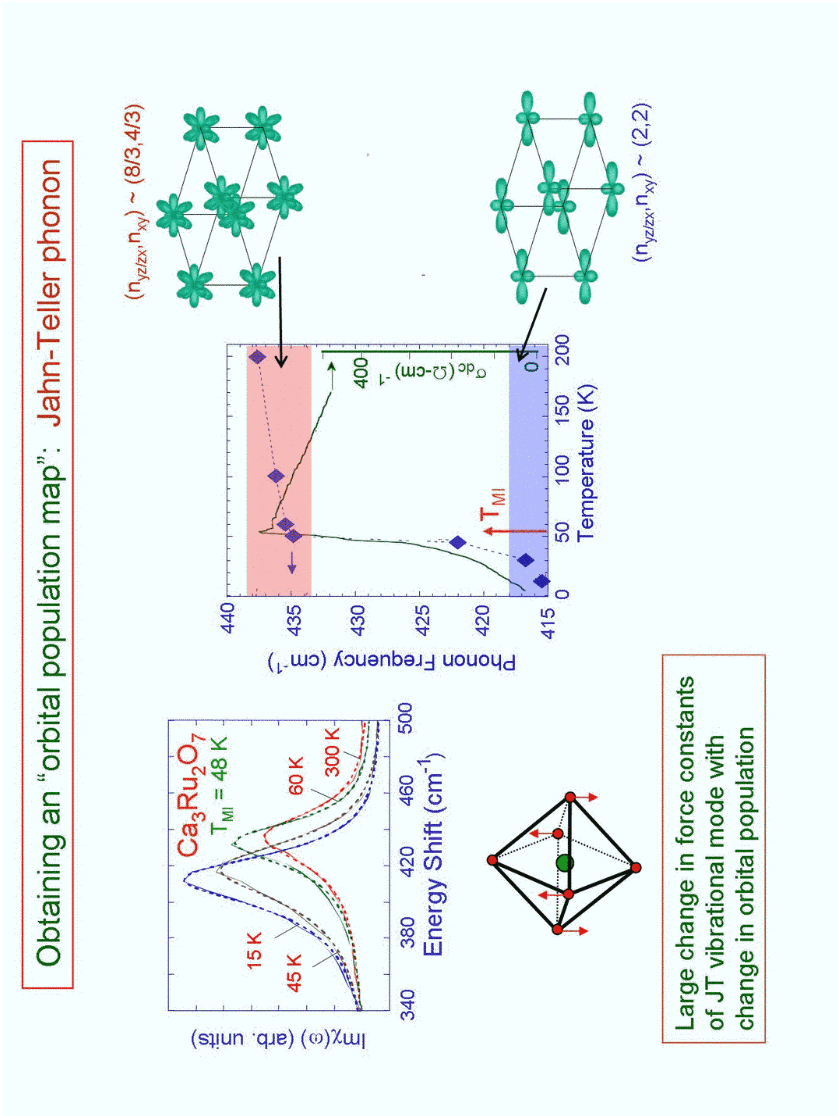

Obtaining an "orbital population map": Jahn-Teller phonon
$(n_{yz/zx}, n_{xy}) \sim (8/3, 4/3)$
$(n_{yz/zx}, n_{xy}) \sim (2, 2)$
$Ca_3Ru_2O_7$
T_{MI} = 48 K
15 K
45 K
60 K
300 K
Energy Shift (cm^{-1})
Imχ(ω) (arb. units)
Phonon Frequency (cm^{-1})
Temperature (K)
σ_{dc} $(\Omega\text{-cm})^{-1}$
T_{MI}
Large change in force constants of JT vibrational mode with change in orbital population

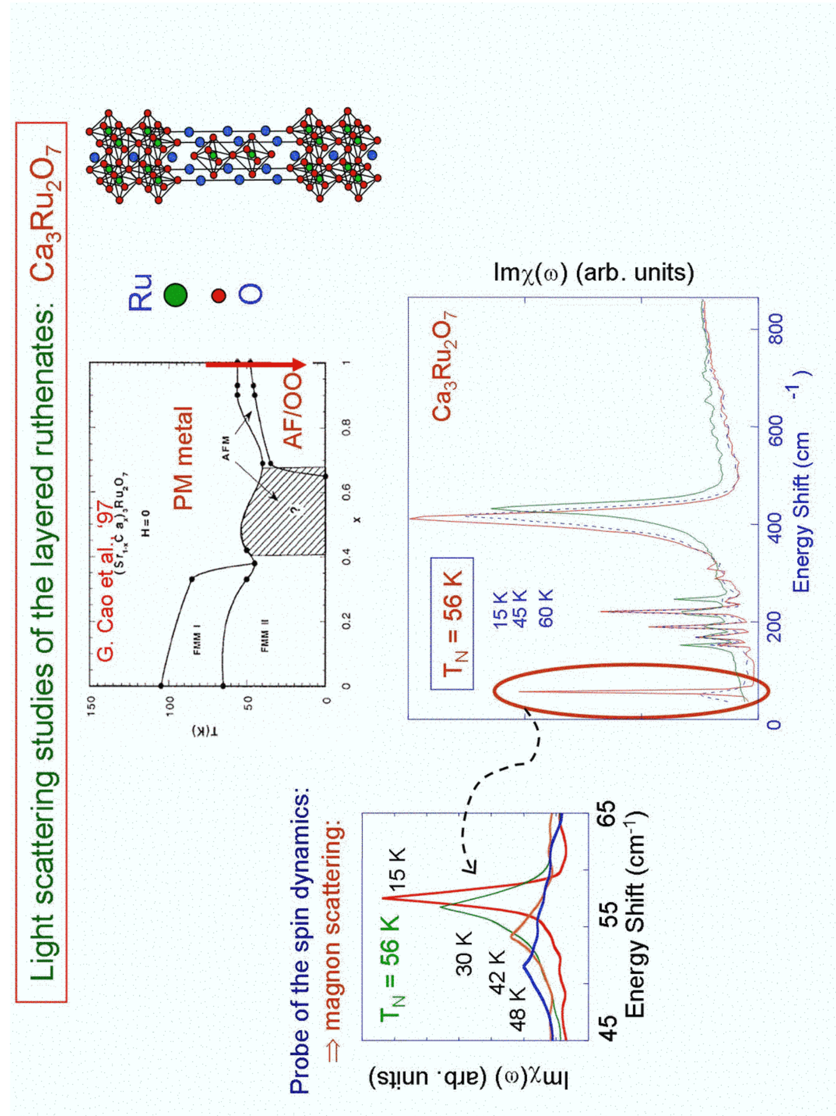

Light scattering studies of the layered ruthenates: $Ca_3Ru_2O_7$
Ru
O
G. Cao et al. '97
PM metal
AF/OO
Imχ(ω) (arb. units)
$Ca_3Ru_2O_7$
T_N = 56 K
15 K
45 K
60 K
Energy Shift (cm^{-1})
Probe of the spin dynamics:
⇒ magnon scattering:
T_N = 56 K
15 K
30 K
42 K
48 K
Energy Shift (cm^{-1})

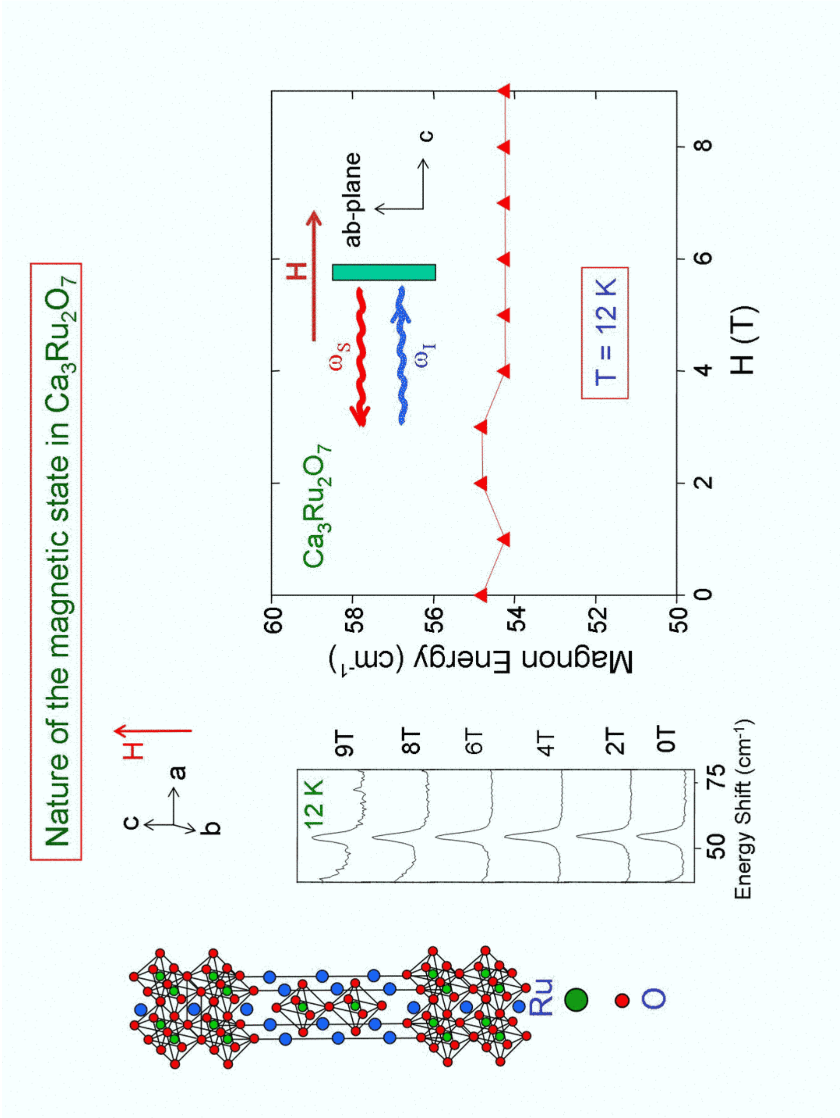
Nature of the magnetic state in $Ca_3Ru_2O_7$
H
c
a
b
Ru
O
12 K
9T
8T
6T
4T
2T
0T
50
75
Energy Shift (cm^{-1})
Magnon Energy (cm^{-1})
$Ca_3Ru_2O_7$
H
ab-plane
c
ω_S
ω_I
T = 12 K
H (T)

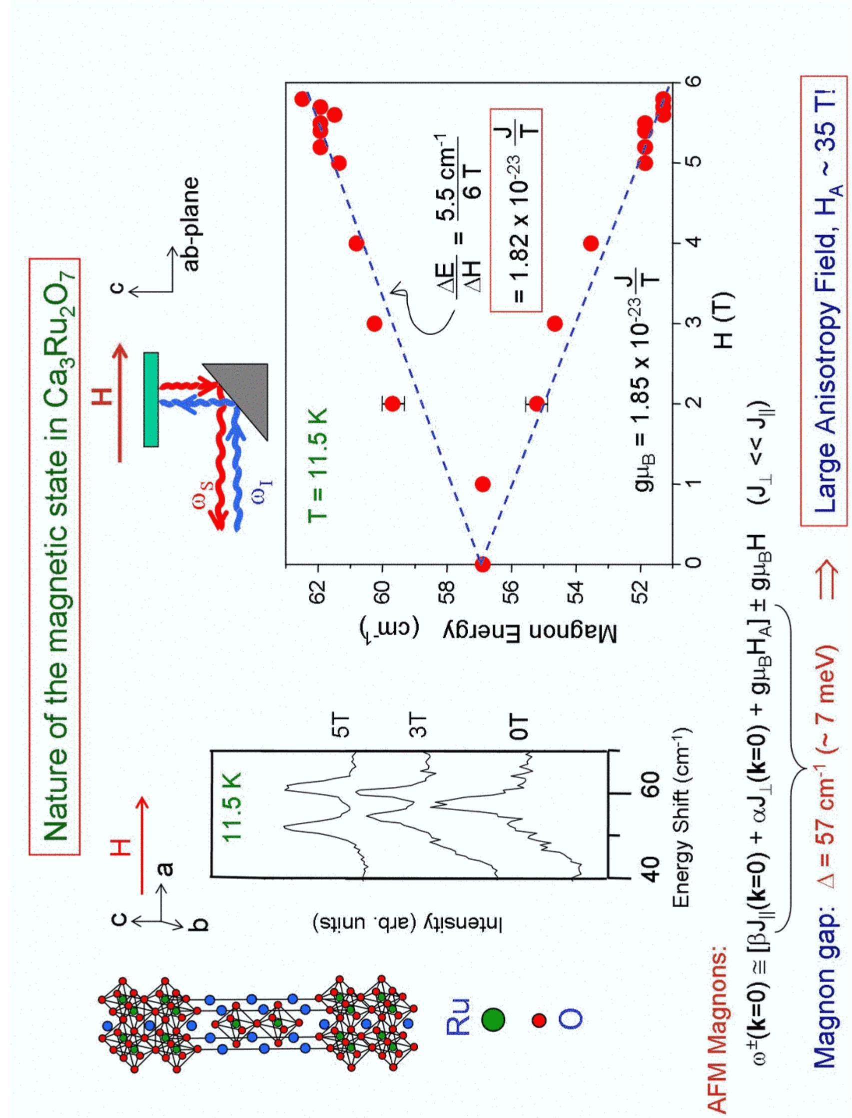
Nature of the magnetic state in $Ca_3Ru_2O_7$
c
a
b
H
11.5 K
5T
3T
0T
Intensity (arb. units)
40
60
Energy Shift (cm^{-1})
Ru
O
H
c
ab-plane
ω_S
ω_I
T = 11.5 K
Magnon Energy (cm^{-1})
$\frac{\Delta E}{\Delta H} = \frac{5.5\ cm^{-1}}{6\ T}$
$= 1.82 \times 10^{-23}\ \frac{J}{T}$
$g\mu_B = 1.85 \times 10^{-23}\ \frac{J}{T}$
H (T)
AFM Magnons:
$\omega^{\pm}(\mathbf{k}=0) \cong [\beta J_{\parallel}(\mathbf{k}=0) + \alpha J_{\perp}(\mathbf{k}=0) + g\mu_B H_A] \pm g\mu_B H$ $(J_{\perp} << J_{\parallel})$
Magnon gap: Δ = 57 cm^{-1} (~ 7 meV) $\Longrightarrow$ Large Anisotropy Field, H_A ~ 35 T!

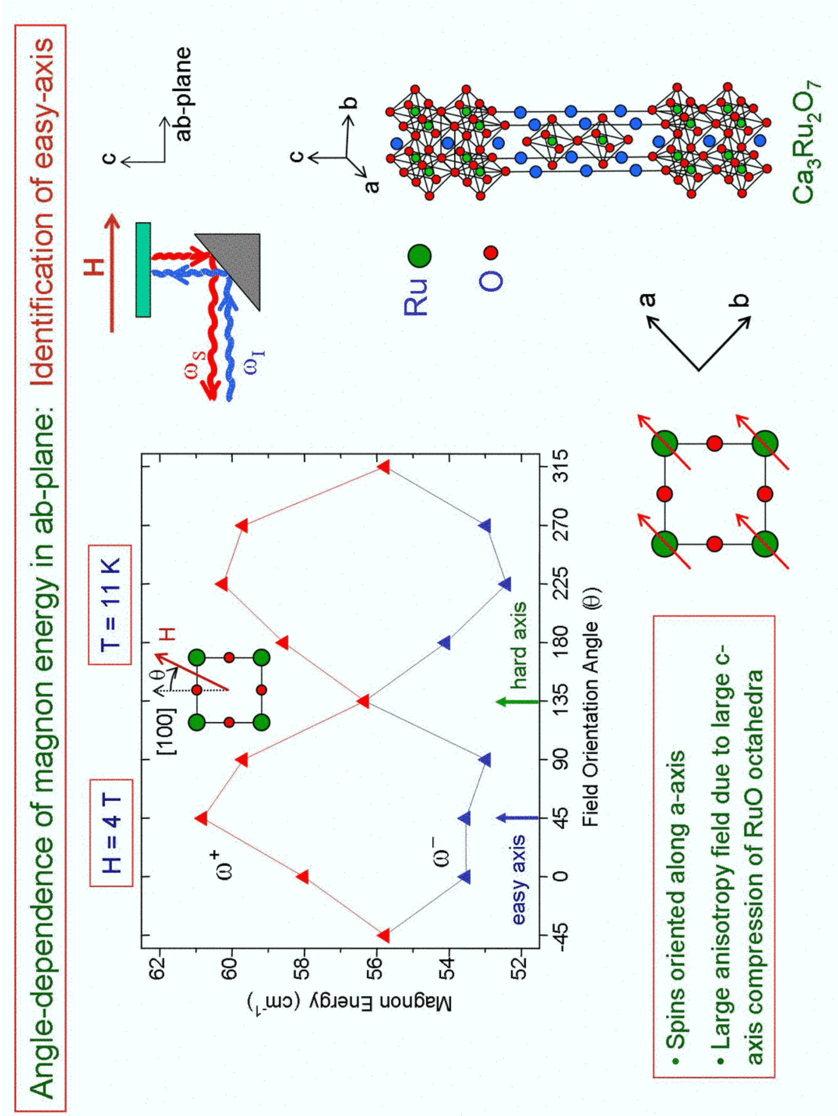
Angle-dependence of magnon energy in ab-plane: Identification of easy-axis
H = 4 T
T = 11 K
Magnon Energy (cm-1)
Field Orientation Angle (θ)
ω+
ω−
easy axis
hard axis
[100]
H
ab-plane
Ru
O
Ca3Ru2O7
• Spins oriented along a-axis
• Large anisotropy field due to large c-axis compression of RuO octahedra

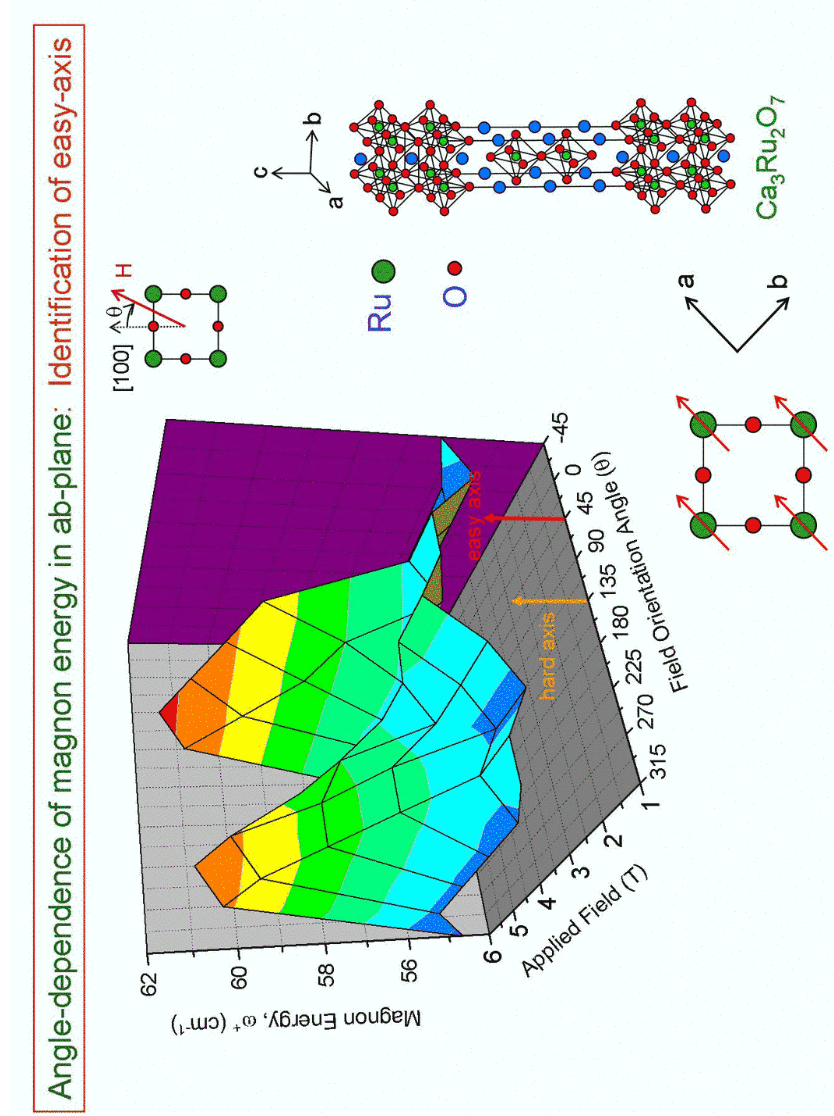
Angle-dependence of magnon energy in ab-plane: Identification of easy-axis
Magnon Energy, ω+ (cm-1)
Applied Field (T)
Field Orientation Angle (θ)
easy axis
hard axis
[100]
H
Ru
O
Ca3Ru2O7

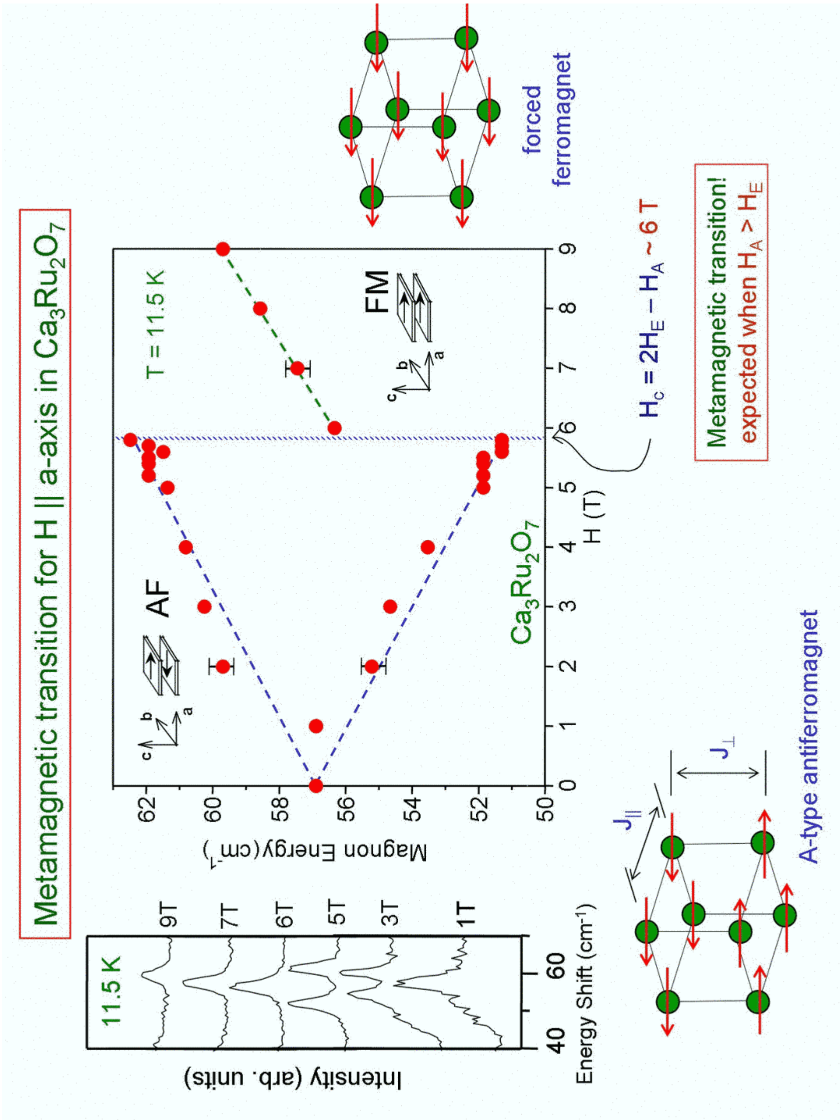
Metamagnetic transition for H || a-axis in $Ca_3Ru_2O_7$
11.5 K
9T
7T
6T
5T
3T
1T
Intensity (arb. units)
Energy Shift (cm^{-1})
Magnon Energy (cm^{-1})
H (T)
T = 11.5 K
AF
FM
$Ca_3Ru_2O_7$
$H_c = 2H_E - H_A \sim 6$ T
Metamagnetic transition!
expected when $H_A > H_E$
forced ferromagnet
A-type antiferromagnet
$J_{||}$
$J_{\perp}$

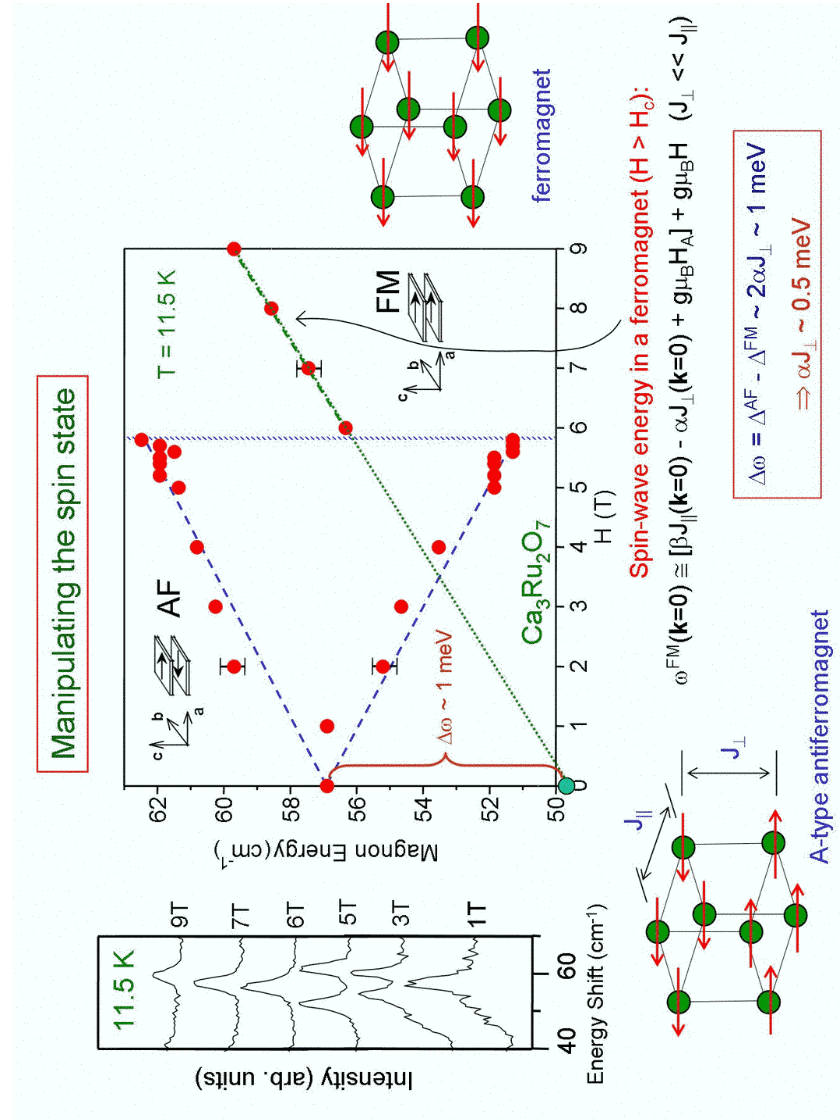
Manipulating the spin state
11.5 K
9T
7T
6T
5T
3T
1T
Intensity (arb. units)
Energy Shift (cm^{-1})
Magnon Energy (cm^{-1})
H (T)
T = 11.5 K
AF
FM
$Ca_3Ru_2O_7$
$\Delta\omega \sim 1$ meV
Spin-wave energy in a ferromagnet ($H > H_c$):
$\omega^{FM}(\mathbf{k=0}) \cong [\beta J_{||}(\mathbf{k=0}) - \alpha J_{\perp}(\mathbf{k=0}) + g\mu_B H_A] + g\mu_B H \quad (J_{\perp} << J_{||})$
$\Delta\omega = \Delta^{AF} - \Delta^{FM} \sim 2\alpha J_{\perp} \sim 1$ meV
$\Rightarrow \alpha J_{\perp} \sim 0.5$ meV
ferromagnet
A-type antiferromagnet
$J_{||}$
$J_{\perp}$

Manipulating the orbital population w/ a magnetic field: H || a-axis

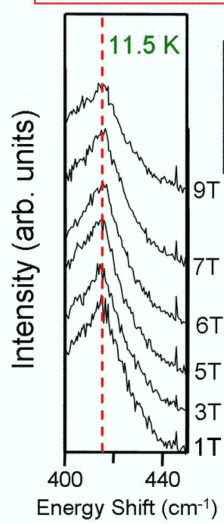

No change in orbital state through the metamagnetic transition – no change in spin direction, and hence no change in spin-orbit energy

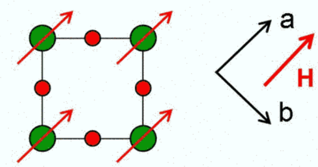

$H_A > H_E$

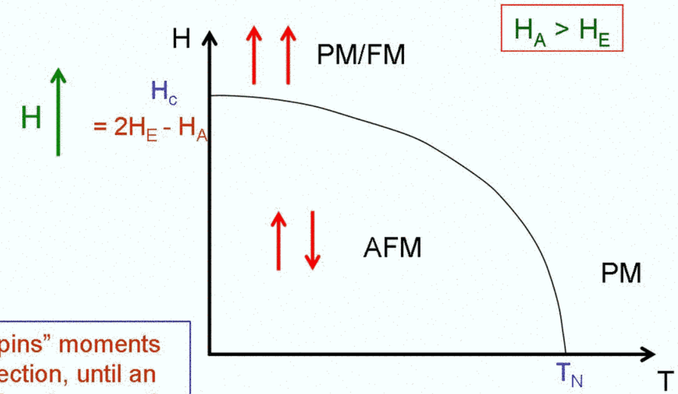

Anisotropy field “pins” moments in a particular direction, until an abrupt AFM – FM metamagnetic transition occurs

Manipulating the orbital population in strongly correlated systems

Two ways to manipulate the orbital population:

(1). ‘Frustrate’ Jahn Teller distortions with pressure

⇒ Hydrostatic pressure favors lower volume, undistorted configuration of octahedra

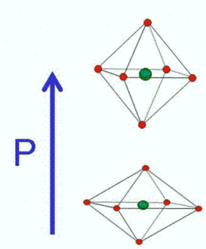

(2). Reorient the atomic moments with a magnetic field

⇒ Orbital rearrangements will result via the strong spin-orbit interaction

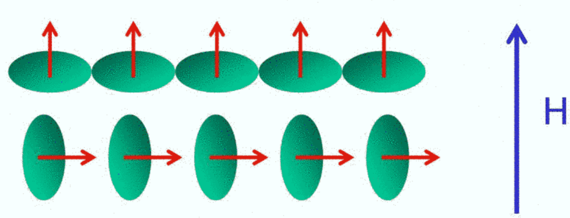

Pressure-induced collapse of the AF phase: $Ca_3Ru_2O_7$

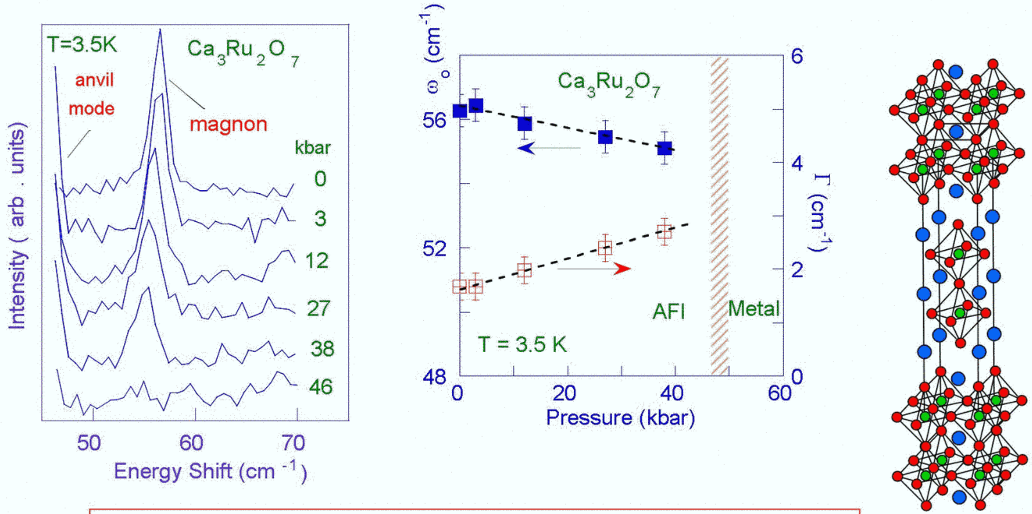

Key points:

- Antiferromagnetism suppressed with pressure
- Decreased H_A and magnon lifetime with pressure
  Not a continuous phase transition! First order!

Pressure-dependence of J in Mott-Hubbard systems: La_2CuO_4 and NiO

La_2CuO_4:

NiO:

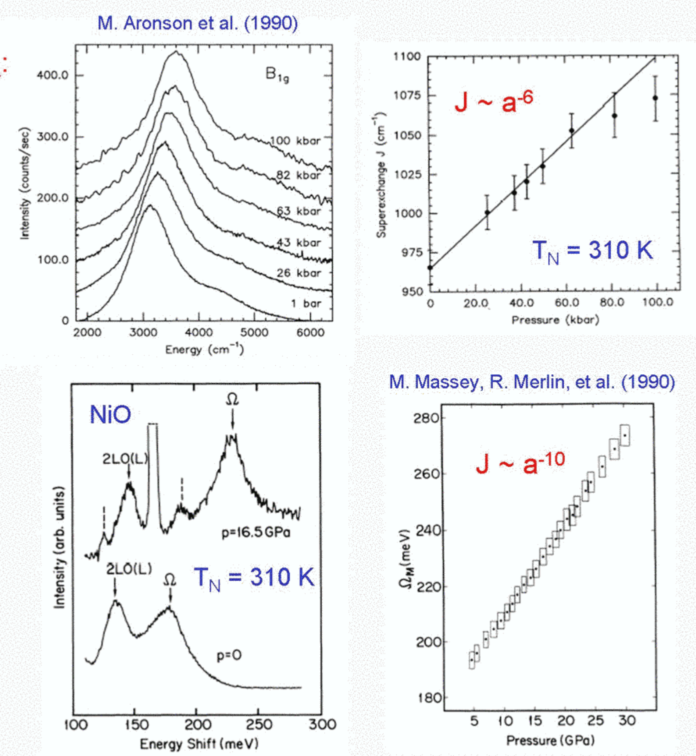

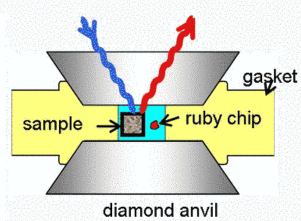

$J \sim t^2/U$

→ $J \sim a^{-\gamma}$

t: hopping parameter
U: Coulomb int.
a: lattice parameter

Pressure stabilizes antiferromagnetism and T_N in "classic" Mott insulators!

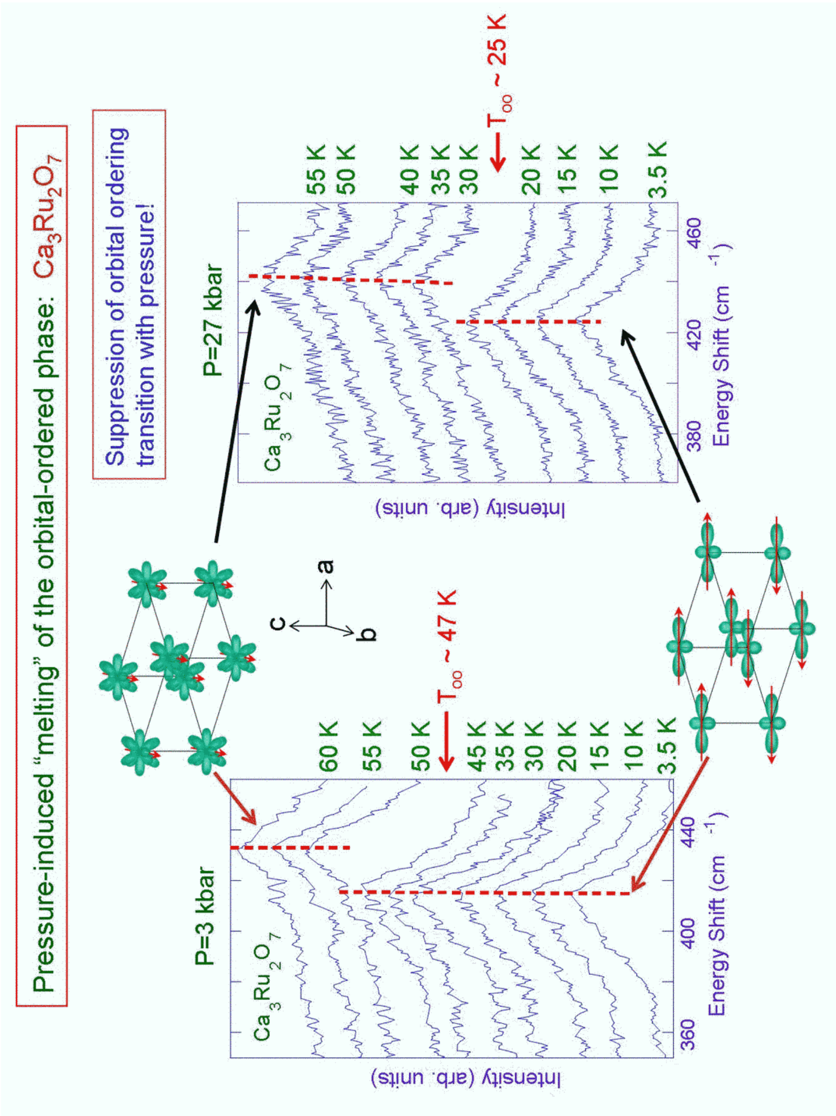
Pressure-induced "melting" of the orbital-ordered phase: $Ca_3Ru_2O_7$
Suppression of orbital ordering transition with pressure!
P=3 kbar
$Ca_3Ru_2O_7$
60 K
55 K
50 K
45 K
35 K
30 K
20 K
15 K
10 K
3.5 K
T_{oo} ~ 47 K
P=27 kbar
55 K
50 K
40 K
35 K
30 K
20 K
15 K
10 K
3.5 K
T_{oo} ~ 25 K
Intensity (arb. units)
Energy Shift (cm^{-1})
c
a
b

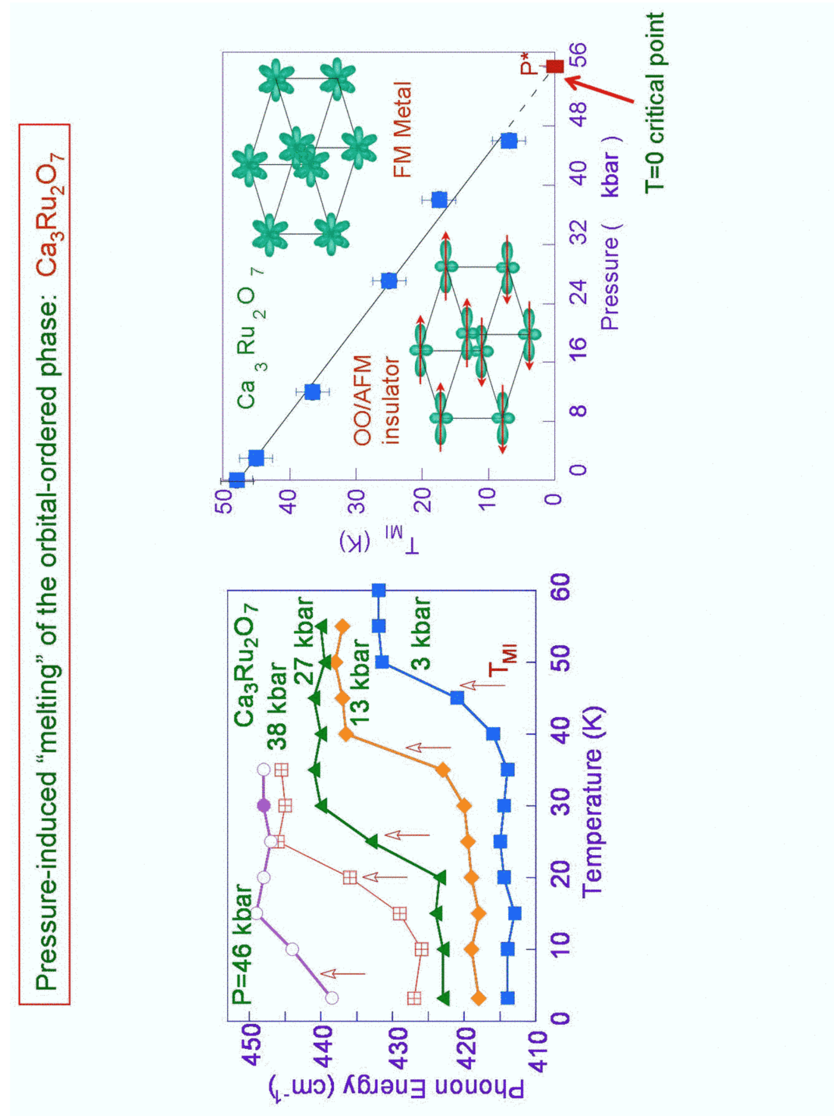
Pressure-induced "melting" of the orbital-ordered phase: $Ca_3Ru_2O_7$
$Ca_3Ru_2O_7$
P=46 kbar
38 kbar
27 kbar
13 kbar
3 kbar
T_{MI}
Phonon Energy (cm^{-1})
Temperature (K)
OO/AFM insulator
FM Metal
P*
T=0 critical point
T_{MI} (K)
Pressure (kbar)

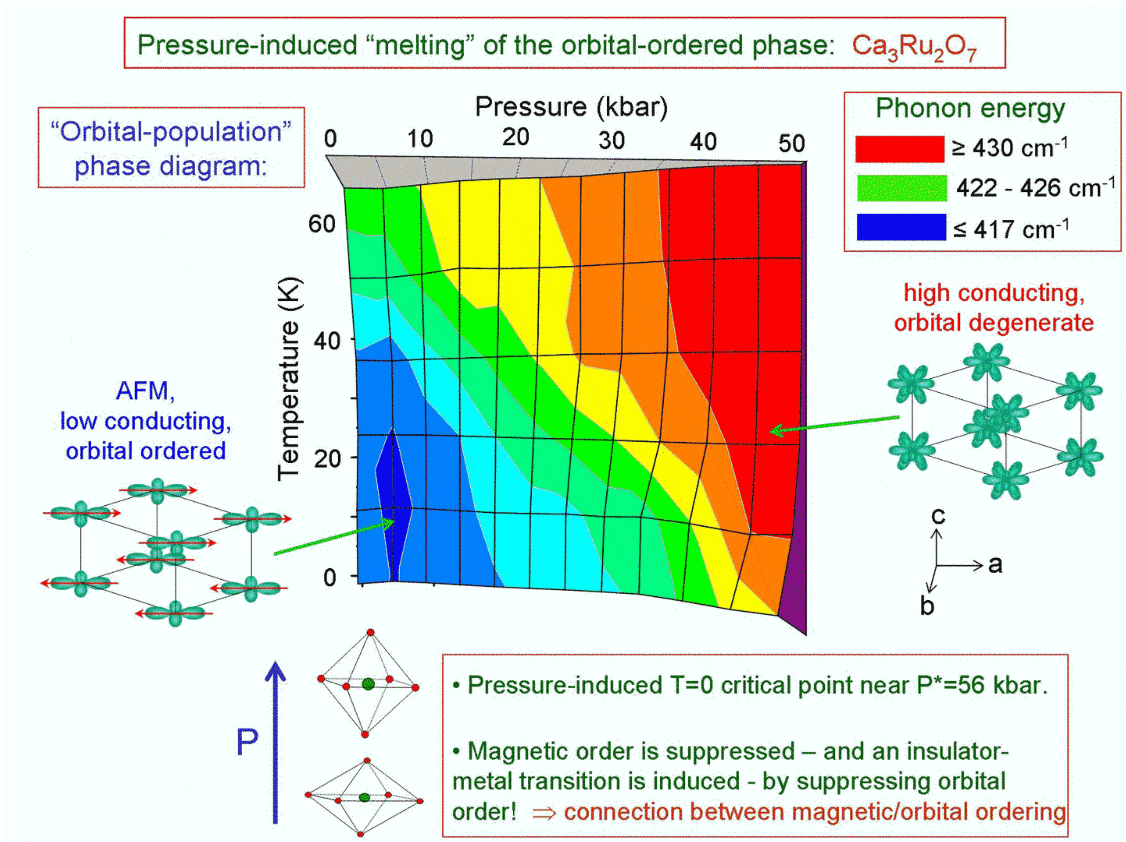
Pressure-induced “melting” of the orbital-ordered phase: $Ca_3Ru_2O_7$
“Orbital-population” phase diagram:
Pressure (kbar)
Temperature (K)
Phonon energy
≥ 430 cm^{-1}
422 - 426 cm^{-1}
≤ 417 cm^{-1}
high conducting, orbital degenerate
AFM, low conducting, orbital ordered
c
a
b
P
• Pressure-induced T=0 critical point near P*=56 kbar.
• Magnetic order is suppressed – and an insulator-metal transition is induced - by suppressing orbital order! ⇒ connection between magnetic/orbital ordering

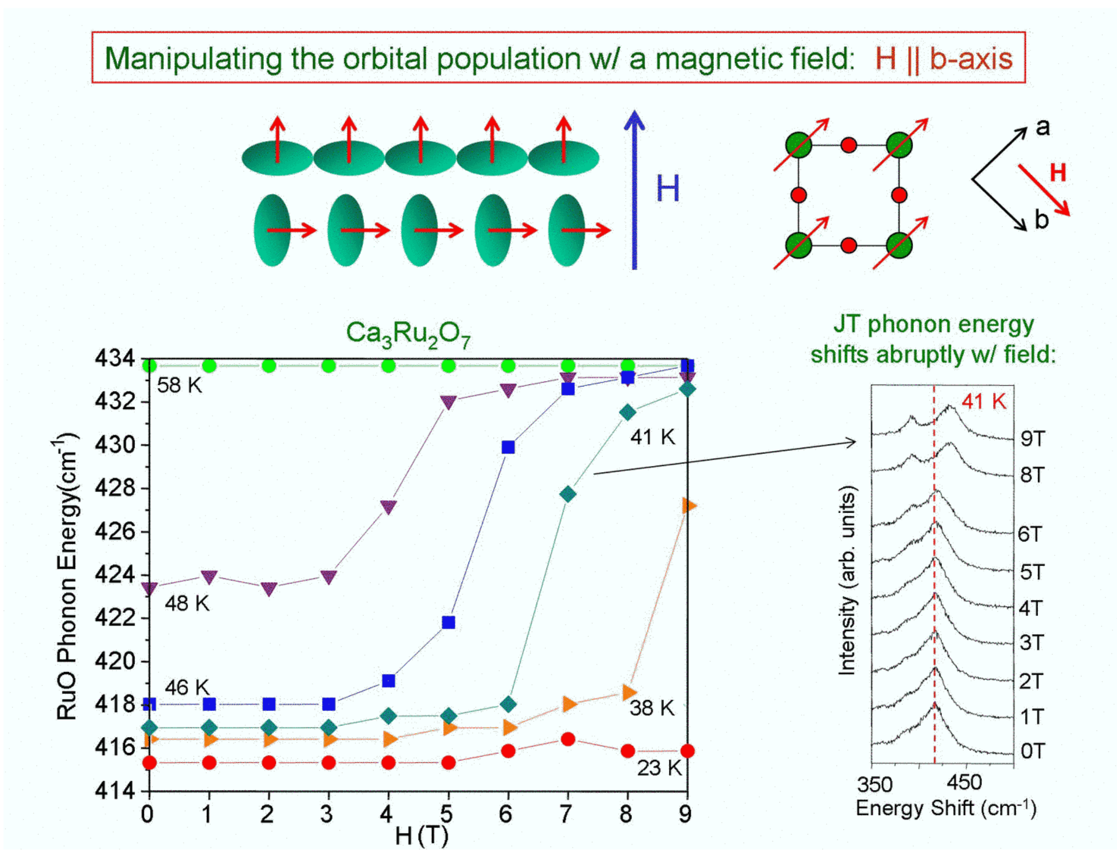
Manipulating the orbital population w/ a magnetic field: H || b-axis
H
a
b
$Ca_3Ru_2O_7$
RuO Phonon Energy(cm^{-1})
H (T)
58 K
48 K
46 K
41 K
38 K
23 K
JT phonon energy shifts abruptly w/ field:
41 K
9T
8T
6T
5T
4T
3T
2T
1T
0T
Intensity (arb. units)
Energy Shift (cm^{-1})

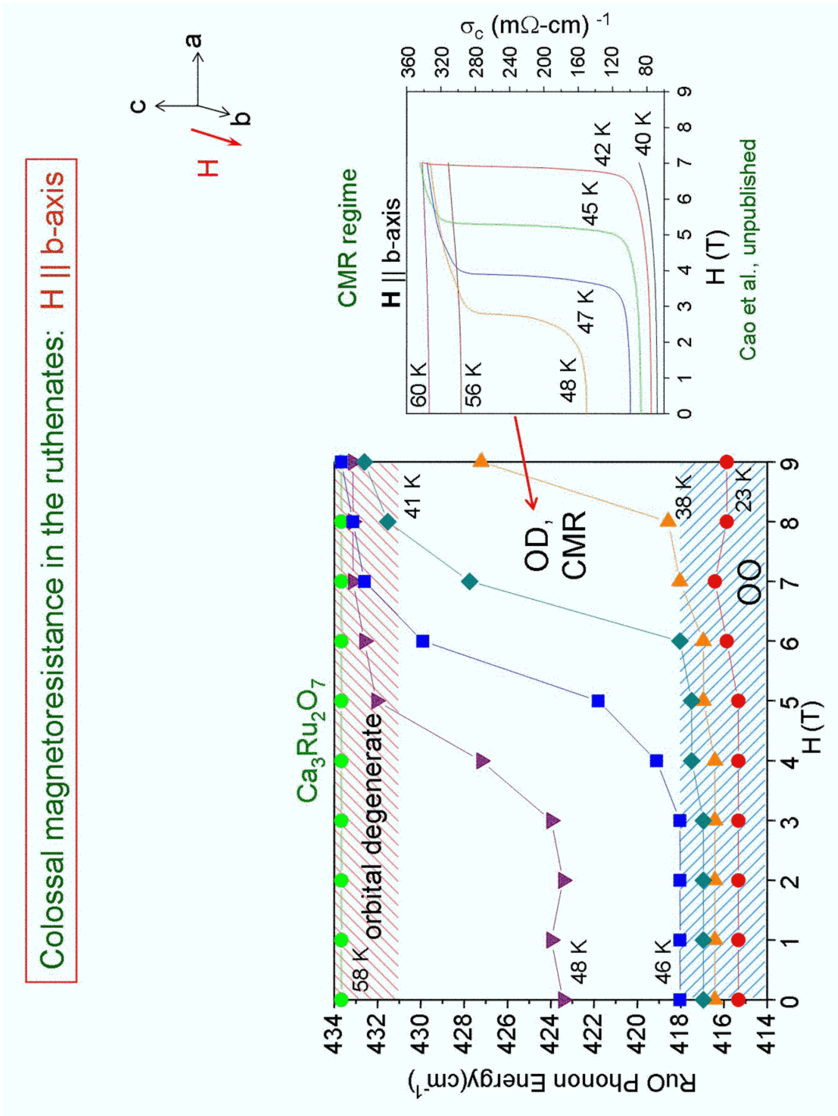
Colossal magnetoresistance in the ruthenates: H || b-axis
H
c
a
b
Ca3Ru2O7
orbital degenerate
OD,
CMR
OO
58 K
48 K
46 K
41 K
38 K
23 K
RuO Phonon Energy(cm-1)
H(T)
CMR regime
H || b-axis
σc (mΩ-cm) -1
60 K
56 K
48 K
47 K
45 K
42 K
40 K
H (T)
Cao et al., unpublished

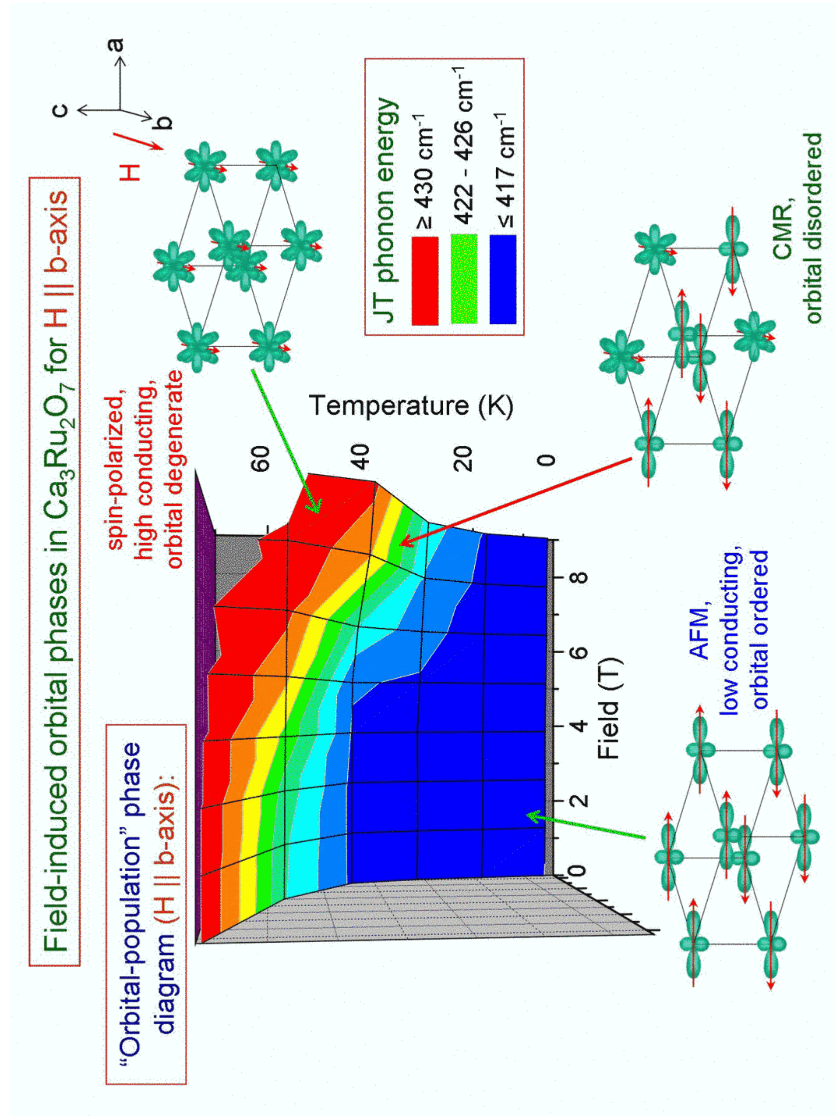
Field-induced orbital phases in Ca3Ru2O7 for H || b-axis
"Orbital-population" phase
diagram (H || b-axis):
H
c
a
b
spin-polarized,
high conducting,
orbital degenerate
JT phonon energy
≥ 430 cm-1
422 - 426 cm-1
≤ 417 cm-1
Temperature (K)
Field (T)
CMR,
orbital disordered
AFM,
low conducting,
orbital ordered

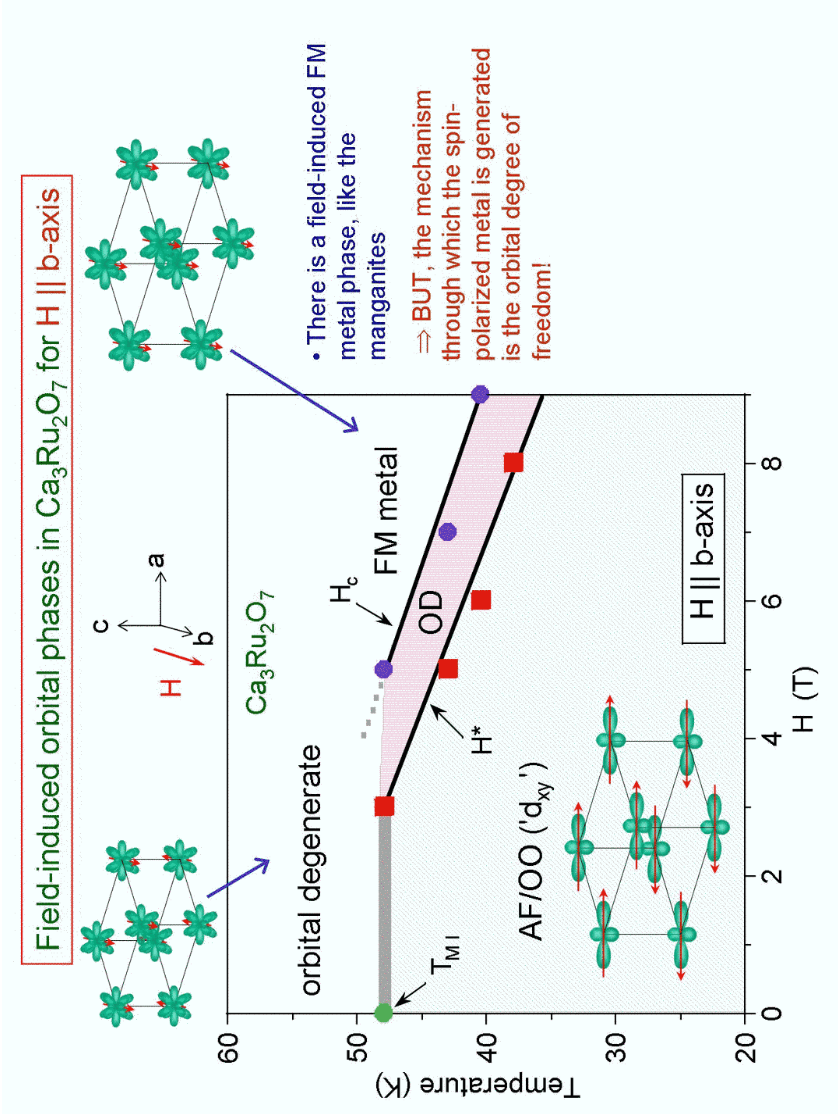
Field-induced orbital phases in Ca3Ru2O7 for H || b-axis
c
a
b
H
Ca3Ru2O7
orbital degenerate
FM metal
OD
Hc
H*
TMI
AF/OO ('dxy')
H || b-axis
Temperature (K)
H (T)
• There is a field-induced FM metal phase, like the manganites
⇒ BUT, the mechanism through which the spin-polarized metal is generated is the orbital degree of freedom!

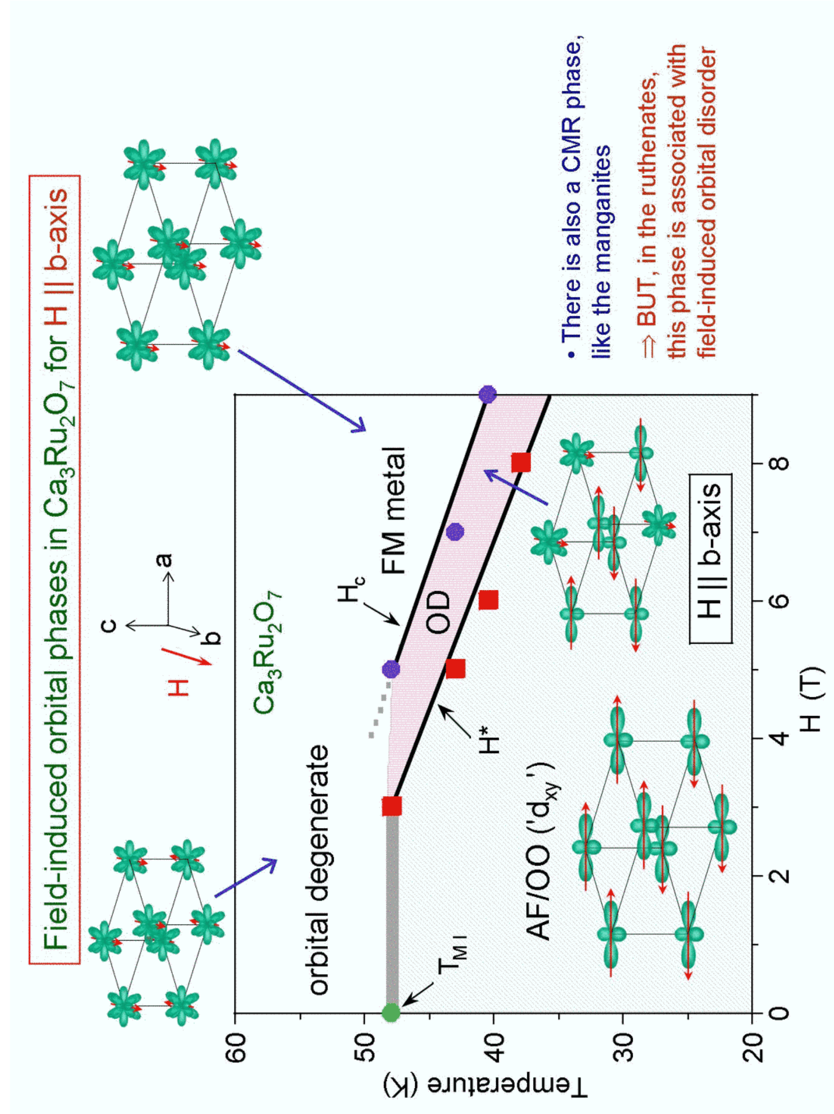
Field-induced orbital phases in Ca3Ru2O7 for H || b-axis
c
a
b
H
Ca3Ru2O7
orbital degenerate
FM metal
OD
Hc
H*
TMI
AF/OO ('dxy')
H || b-axis
Temperature (K)
H (T)
• There is also a CMR phase, like the manganites
⇒ BUT, in the ruthenates, this phase is associated with field-induced orbital disorder

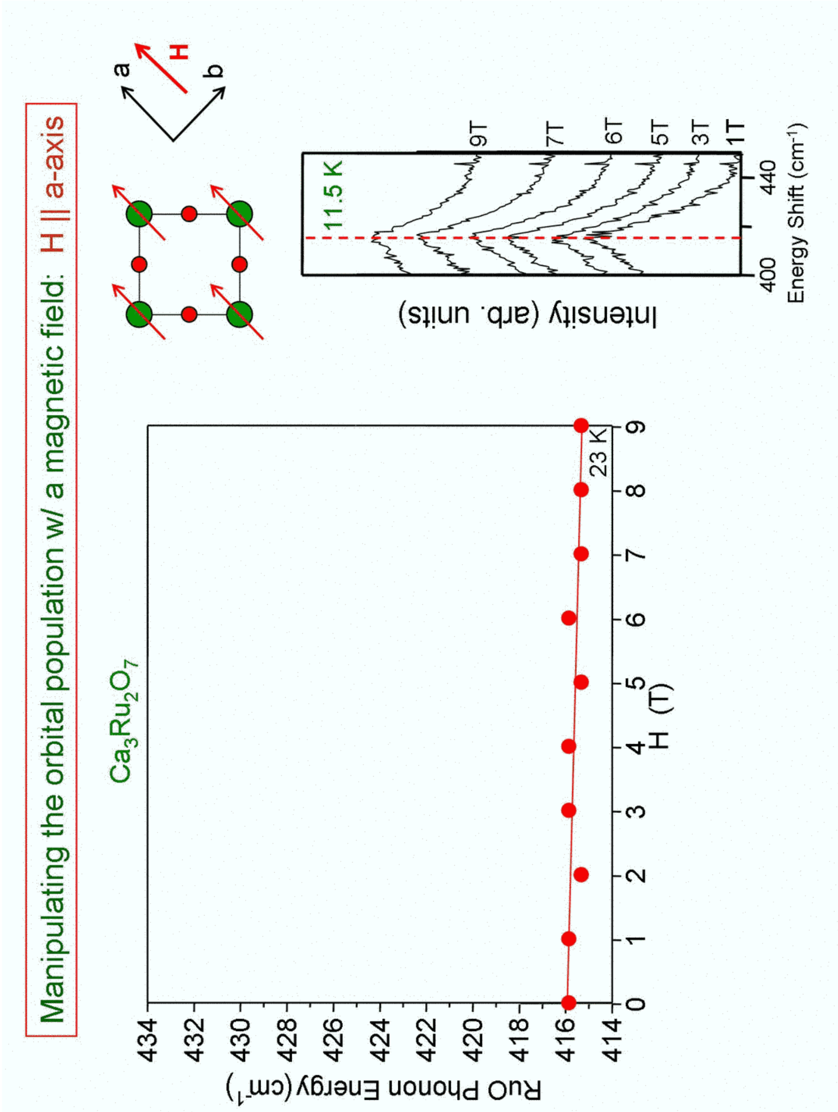
Manipulating the orbital population w/ a magnetic field: H || a-axis
Ca3Ru2O7
a
b
H
11.5 K
9T
7T
6T
5T
3T
1T
Intensity (arb. units)
Energy Shift (cm-1)
400
440
23 K
RuO Phonon Energy (cm-1)
H (T)

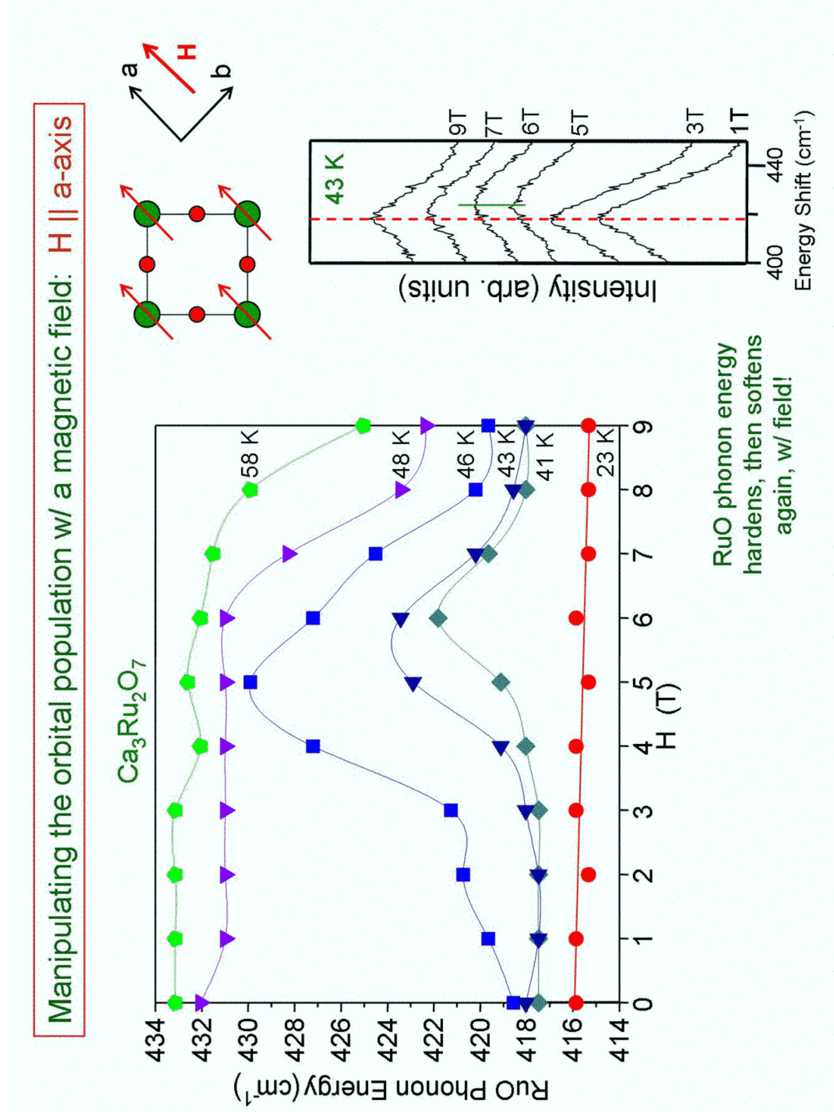
Manipulating the orbital population w/ a magnetic field: H || a-axis
Ca3Ru2O7
a
b
H
43 K
9T
7T
6T
5T
3T
1T
Intensity (arb. units)
Energy Shift (cm-1)
400
440
58 K
48 K
46 K
43 K
41 K
23 K
RuO Phonon Energy (cm-1)
H (T)
RuO phonon energy hardens, then softens again, w/ field!

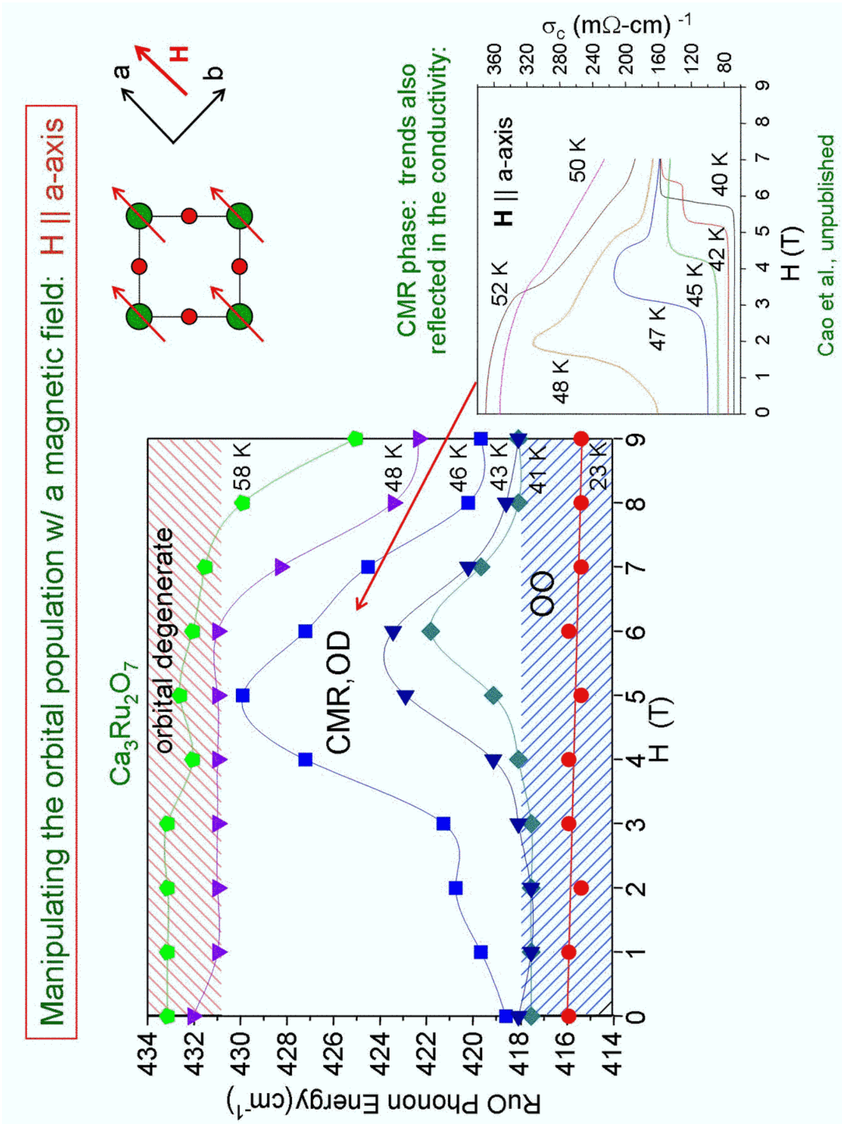
Manipulating the orbital population w/ a magnetic field: H || a-axis
a
b
H
$Ca_3Ru_2O_7$
orbital degenerate
CMR,OD
OO
58 K
48 K
46 K
43 K
41 K
23 K
RuO Phonon Energy (cm^{-1})
H (T)
CMR phase: trends also reflected in the conductivity:
σ_c (mΩ-cm)$^{-1}$
H || a-axis
52 K
50 K
48 K
47 K
45 K
42 K
40 K
Cao et al., unpublished

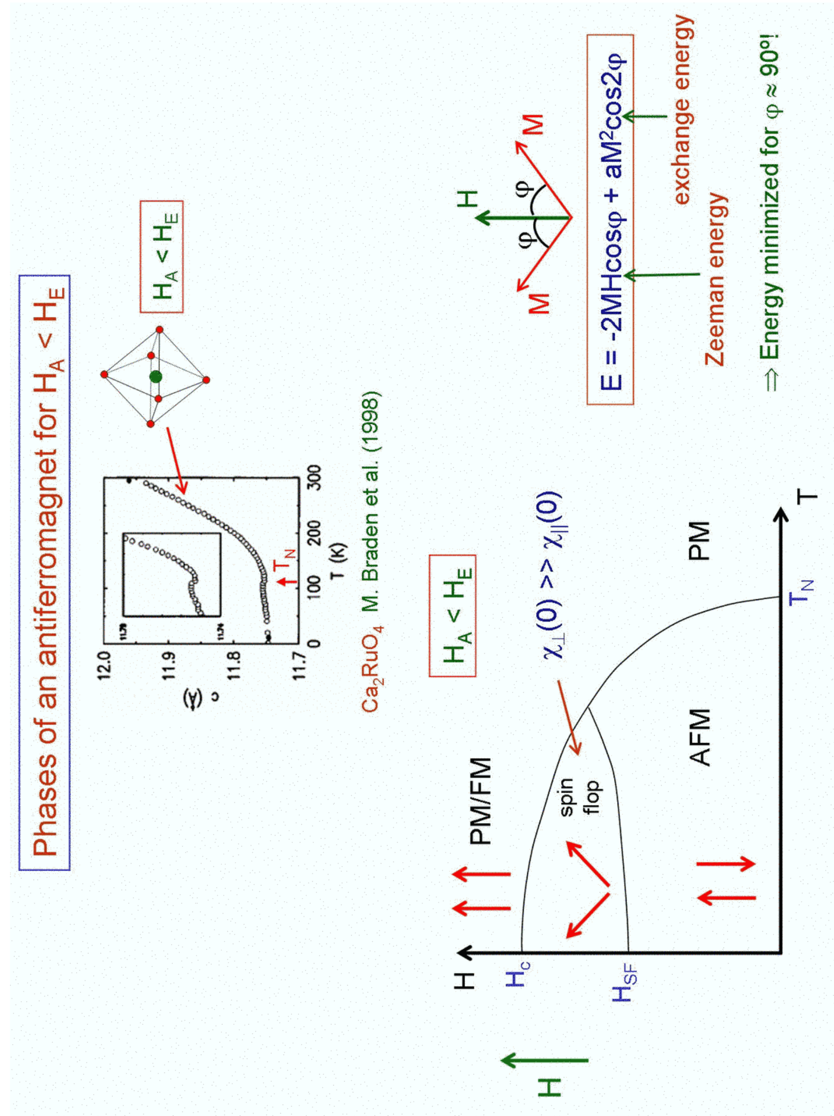
Phases of an antiferromagnet for $H_A < H_E$
$H_A < H_E$
T (K)
T_N
Ca_2RuO_4 M. Braden et al. (1998)
$\chi_\perp(0) >> \chi_{||}(0)$
PM/FM
spin flop
AFM
PM
H
T
H_c
H_{SF}
T_N
M
φ
$E = -2MH\cos\varphi + aM^2\cos2\varphi$
exchange energy
Zeeman energy
$\Rightarrow$ Energy minimized for $\varphi \approx 90°$!

Field-induced orbital phases in $Ca_3Ru_2O_7$ for H || a-axis

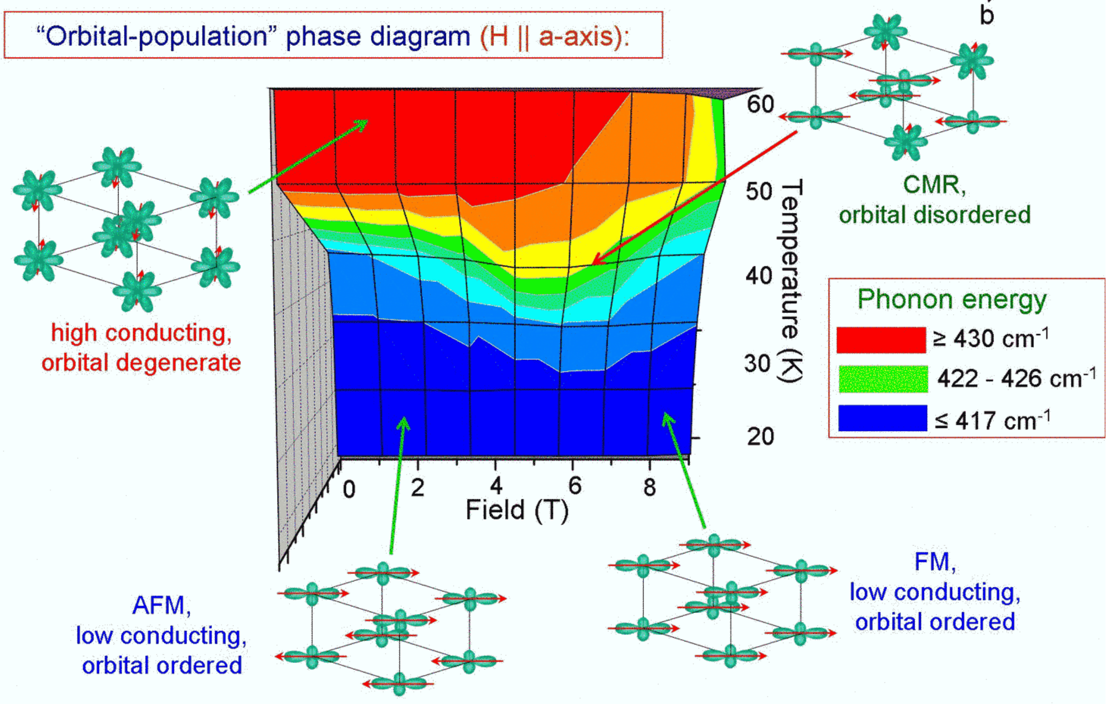

Field-induced orbital phases in $Ca_3Ru_2O_7$ for H || a-axis

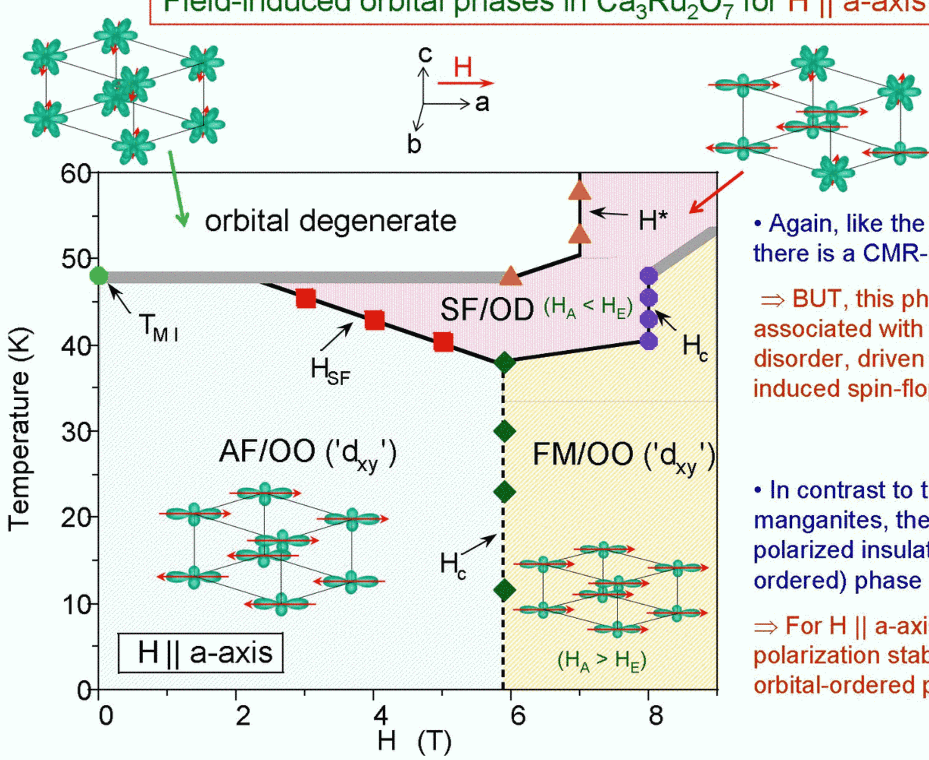

- Again, like the manganites, there is a CMR-like phase

⇒ BUT, this phase is associated with orbital disorder, driven by a field-induced spin-flop phase

- In contrast to the manganites, there is a spin-polarized insulating (orbital-ordered) phase

⇒ For H || a-axis, spin polarization stabilizes the orbital-ordered phase!

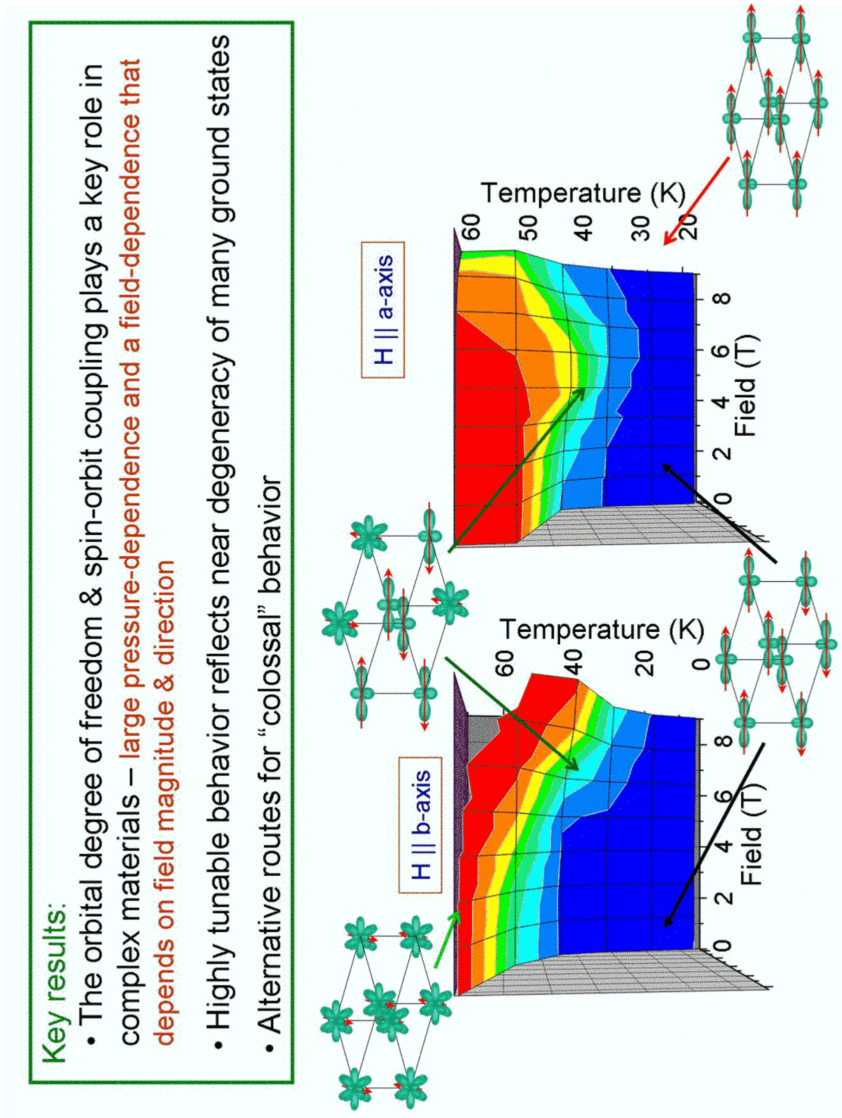
Key results:
• The orbital degree of freedom & spin-orbit coupling plays a key role in complex materials – large pressure-dependence and a field-dependence that depends on field magnitude & direction
• Highly tunable behavior reflects near degeneracy of many ground states
• Alternative routes for "colossal" behavior
H || b-axis
Temperature (K)
60
40
20
0
Field (T)
0
2
4
6
8
H || a-axis
Temperature (K)
60
50
40
30
20
Field (T)
0
2
4
6
8